厚生労働科学研究研究費補助金
萌芽的先端医療技術推進研究事業

薬物トランスポーターの分子多様性と機能解析および副作用発現との連鎖解析に関する研究

平成１４～１６年度　総合研究報告書(2/2)

主任研究者　杉山　雄一

平成１７（２００５）年３月

ACADEMIC PRESS

Cellular Immunology 215 (2002) 186–194

Cellular Immunology

www.academicpress.com

Human peripheral blood monocyte-derived interleukin-10-induced semi-mature dendritic cells induce anergic $CD4^+$ and $CD8^+$ T cells via presentation of the internalized soluble antigen and cross-presentation of the phagocytosed necrotic cellular fragments

Katsuaki Sato,[a,*] Naohide Yamashita,[b] and Takami Matsuyama[a]

[a] *Department of Immunology and Medical Zoology, School of Medicine, Kagoshima University, 8-35-1 Sakuragaoka, Kagoshima City, Kagoshima 890-8520, Japan*

[b] *The Institute of Medical Science, The University of Tokyo, 4-6-1 Shirokanedai, Minato-ku, Tokyo 108-8639, Japan*

Received 17 January 2002; accepted 9 May 2002

Abstract

We examined the ability of human monocyte-derived interleukin (IL)-10-induced semi-mature dendritic cells (semi-mDCs) that had been pulsed with soluble protein and necrotic cellular fragments to induce an antigen (Ag)-specific anergy in $CD4^+$ and $CD8^+$ T cells. IL-10 converted normal immature DCs (iDCs) into semi-mDCs during the maturation. In contrast to normal iDCs and mature DCs, IL-10-induced semi-mDCs as well as IL-10-treated iDCs not only had reduced their allogeneic T cell-stimulatory capacity, but also induced an allogeneic Ag-specific anergy in T cells. Normal mDCs that had been pulsed with tetanus toxin (TT) or allogeneic necrotic cellular fragments caused further activation of TT-specific $CD4^+$ T cells or allogeneic fibroblast-specific $CD8^+$ T cells. Ag-pulsed IL-10-induced semi-mDCs induced an anergic state in both cell types. Thus, our results suggest that IL-10-induced semi-mDCs induce an Ag-specific anergy in $CD4^+$ and $CD8^+$ T cells via presentation of the internalized protein and cross-presentation of the phagocytosed cellular fragments. © 2002 Elsevier Science (USA). All rights reserved.

Keywords: DCs; Antigen presentation; IL-10; Antigen-specific T cells; Anergy

1. Introduction

Dendritic cells (DCs)[1] are unique professional antigen (Ag)-presenting cells (APCs) capable of stimulating naïve T cells as part of the primary immune response, and are more potent APCs than monocytes/macrophages or B cells [1–3]. DCs take up exogenous soluble protein Ags via macropinocytosis, and present them to $CD4^+$ T helper (Th) cells via the MHC class II-restricted pathway [4,5]. On the other hand, DCs also acquire soluble proteins by macropinocytosis for presentation to $CD8^+$ cytotoxic T (Tc) cells in the MHC class I-restricted pathway [4,5]. Similarly, DCs can take up Ag released from cells undergoing necrosis or apoptosis for presentation to MHC class I-restricted Tc cells, a process referred to as cross-presentation [4,5].

Interleukin (IL)-10 is a multifunctional cytokine produced by activated T cells, B cells, keratinocytes, monocytes/macrophages, DCs, and certain tumor cells [6–10]. IL-10 has been shown to inhibit activation and proliferation of human peripheral blood (PB) T cells

* Corresponding author. Fax: +81-99-275-5305.
E-mail address: katsuaki@m3.kufm.kagoshima-u.ac.jp (K. Sato).

[1] *Abbreviations used:* Ab, antibody; Ag, antigen; APCs, Ag-presenting cells; CBMCs, cord blood mononuclear cells; DCs, dendritic cells; E/T ratios, effector cell to target cell ratios; FasL, Fas ligand; FITC-OVA, FITC-labeled ovalbumin; GM-CSF, granulocyte-macrophage colony-stimulating factor; iDCs, immature DCs; IFN, interferon; IL, interleukin; LPS, lippolysaccharide; mAb, monoclonal Ab; mDCs, mature DCs; MFI, mean fluorescence intensity; MLR, mixed leukocyte reaction; PB, peripheral blood; PBMCs, peripheral blood mononuclear cells; SD, standard deviation; Tc, cytotoxic T; Th1, type-1 T helper; TNF, tumor necrosis factor; Tr, regulatory T; TRAIL, TNF-related apoptosis-inducing ligand; TT, tetanus toxin.

0008-8749/02/$ - see front matter © 2002 Elsevier Science (USA). All rights reserved.
PII: S0008-8749(02)00021-7

following extracellular stimulation [7]. IL-10 also inhibits T cell stimulatory capacity of DCs as well as monocytes/macrophages via downregulation of MHC and costimulatory molecules [8–10]. Steinbrink et al. [8,9] have reported that treatment of immature DCs (iDCs), but not mature DCs (mDCs), with IL-10 not only reduced their allogeneic T cell-stimulatory capacity, but also induced an allogeneic Ag-specific anergy in T cells. In addition, antigenic peptide-pulsed IL-10-treated DCs also caused an Ag-specific anergy in Th and Tc cells [8,9].

To address whether IL-10-induced semi-mature DCs (semi-mDCs) negatively regulate the function of Ag-specific effector T cells via presentation of the internalized soluble antigenic protein and cross-presentation of the phagocytosed necrotic cells, we examined the ability of human IL-10-induced semi-mDCs that had been pulsed with protein and cellular fragments derived from necrotic cells to induce an anergic state in Ag-specific $CD4^+$ and $CD8^+$ T cells.

2. Materials and methods

2.1. Media and reagents

The medium used throughout was RPMI 1640 (Sigma, St. Louis, MO) supplemented with antibiotic–antimycotic (GIBCO BRL, Rockville, MD) and 10% heat inactivated FCS (GIBCO). Granulocyte-macrophage colony-stimulating factor (GM-CSF), IL-2, IL-4, IL-10, and tumor necrosis factor (TNF)-α were purchased from Pepro Tech. (London, England). Lipopolysaccharide (LPS) (*E. coli* 0127B8) was obtained from Sigma. FITC-labeled ovalbumin (FITC-OVA) was purchased from Molecular Probes (Eugene, OR).

2.2. In vitro generation and culture of human normal and IL-10-treated DCs

Normal iDCs were obtained by culturing PB monocytes with GM-CSF (50 ng/ml) and IL-4 (50 ng/ml) for 7 days [10]. For the preparation of normal mDCs, cells were subsequently cultured with TNF-α (50 ng/ml) or LPS (100 ng/ml) for another 3 days [10]. Alternatively, iDCs were treated with IL-10 (50 ng/ml) for 3 days, and subsequently cultured with TNF-α (50 ng/ml) or LPS (100 ng/ml) for 3 days. Cell differentiation was monitored by light microscopy, and the resultant cells were used for subsequent experiments. For preparation of Ag-pulsed APCs, normal or IL-10-treated iDCs (10^6) were cultured with OVA (1 μg/ml; Sigma), tetanus toxin (TT) (1 μg/ml; Biogenesis, Poole, England), or necrotic allogeneic fibroblasts (10^5; BioWhittaker, Walkersville, MD) [5] for 24 h, and cells were subsequently stimulated with TNF-α (50 ng/ml) for 3 days.

2.3. Flow cytometry

For surface marker analysis [10], cells were cultured with following monoclonal antibodies (mAbs) conjugated to FITC or PE for direct fluorescein: CD83 (Coulter Immunology, Hialeah, FL), CD4, CD8, CD25, CD40, CD80, CD86, CD152, CD154, HLA-A/B/C, and HLA-DR (BD PharMingen, San Diego, CA). Cells were also stained with the corresponding FITC- or PE-conjugated isotype-matched control mAb (BD PharMingen). Alternatively, intracellular analysis of the expression of cytokines was performed according to the manufacturer's instructions with some modification. In brief, T cells were stimulated with platebound anti-CD3 mAb (10 μg/ml; BD PharMingen) plus soluble anti-CD28 mAb (10 μg/ml; BD PharMingen) for 6 h. Two μM monensin (Sigma) was added for the last 5 h of culture. Cells were collected, washed, fixed, and saponin-permeabilized (fix/perm solution; BD PharMingen), and stained with mAbs to IL-2, IL-4, IL-10, and IFN-γ (BD PharMingen). Analysis of fluorescence staining was performed with a FACS Calibur flow cytometer (Becton Dickinson, Mountain View, CA) and CELLQuest Software, and data are expressed as mean fluorescence intensity (MFI) ± standard deviation (SD) and % mean positivity ±SD.

2.4. Endocytosis assay with FITC-OVA

The methods used to determine the endocytotic activity of DCs have been described previously [10]. Briefly, FITC-OVA was added at a final concentration of 1 μg/ml to the cells (10^6). After incubation for 60 min at 37 °C, cells were washed four times with ice-cold PBS. The uptake by cells was measured by flow cytometry.

2.5. Preparation of T cells

$CD3^+$ T cells were isolated from PB mononuclear cells (PBMCs) or cord blood mononuclear cells (CBMCs) as described previously [11]. Following this procedure, $CD4^+$ T-cell subset was subsequently negatively selected from $CD3^+$ T cells [11]. These T-cell preparations were typically >98% pure as indicated by anti-CD3 mAb and/or anti-CD4 mAb (BD PharMingen) staining.

2.6. Preparation of TT-specific $CD4^+$ T cells and allogeneic fibroblast-specific $CD8^+$ T cells

PBMCs (10^7) were primed with TT (1 μg/ml) or necrotic [5] allogeneic fibroblasts (10^6) for 3 weeks in medium containing IL-2 (100 U/ml) (an induction phase). Following this procedure, $CD4^+$ or $CD8^+$ T cells were negatively selected from the respective Ag-primed PBMCs [11]. The resultant cells (>95% $CD3^+CD4^+$

transplantation (HSCT) are limited to the small population of 8- to 12-Gy uniformly irradiated victims who can receive transplants from an HLA-matched sibling in the early stages of ARS. Development of hematopoietic growth factors (HGF) allowed us the treatment option of administering HGF without HSCT [2].

For overcoming the limitations of BMT, umbilical cord blood (CB) is an ideal stem cell source with a lower incidence and reduced extent of GVHD. It eliminates donor acquisition delay and allows urgent triage for ARS. Accumulating results suggest that use of umbilical CB transplantation (CBT) correlates with a lower incidence of acute and chronic GVHD [3-16], even in the presence of HLA-mismatched donor/recipient parity [5-9,11,12], than is achieved with BMT [10-12]. The feasibility and efficacy of CBT for adult recipients also have been established [13-17]. The increasing numbers of cryopreserved umbilical CB units in local CB banks supplied us the opportunity to identify HLA-compatible donor candidates with sufficient numbers of stem cell doses who would tolerate HLA 1-locus to 3-loci mismatched CBT.

A criticality accident occurred at the uranium fuel processing plant of JCO Co. Ltd. in Tokaimura, Ibaraki Prefecture, Japan, on September 30, 1999 [18]. Fast-neutron radiation was a major component of the accidental irradiation, and the rest was γ-rays. Three employees of JCO were exposed to high radiation doses of 16 to 24.5 GyEq, 6 to 10 GyEq, and 2 to 5 GyEq [19]. We report on the second victim. Accurate dose estimation is essential to determining the strategy for clinical intervention in ARS, although the mixed components of fast neutrons with γ-rays and nonuniform irradiation made estimation difficult. Dosimetry was based on 4 parameters: presence of prodromal symptoms, change in peripheral blood (PB) components, results of PB chromosome analysis, and amount of radioactive ^{24}Na in samples of PB. Our patient started to vomit almost an hour after the exposure [20]. Nausea and vomiting within 1 hour were evaluated as 6- to 8-GyEq radiation according to the International Atomic Energy Agency criteria [2]. The patient's white blood cell (WBC) count 2 to 3 hours after the exposure was 12,700/mm^3, and the lymphocyte subset was only 1% of WBC count. The lymphocyte count reached zero by the seventh day after exposure. The platelet count was 15.9×10^4/mm^3, linearly decreasing from the fifth day after exposure, and decreased to less than 50,000/mm^3 within 10 days. These hematological findings suggested that the patient was irradiated at a dose from 6 to 8 GyEq of radiation. PB ringed chromosome analysis of this patient indicated that the irradiated dose was 7.8 to 8.3 GyEq, and the measurement of radioactive ^{24}Na in the PB samples demonstrated a 9.3-GyEq radiation dose. These findings revealed that the patient had severe impairment of hematopoiesis from high-dose radiation. We therefore determined that it was necessary to perform urgent rescue hematopoiesis by HSCT, despite the nonuniform irradiation. We have previously described the clinical outcome of CBT in this patient [21-23]. Donor/recipient mixed chimerism and unexpected rapid autologous hematopoietic recovery were obtained. However, the recovered autologous hematopoiesis possessed defective immune function, and life-threatening infection and death resulted.

We discuss the clinical intervention strategy for the treatment of ARS, focusing on the immune function of the radiation victim.

2. Materials and Methods

2.1. Patient

The transplantation procedure and clinical course have been previously described [21-23]. Briefly, pretransplantation conditioning consisted of antithymocyte equine γ-globulin alone (2.5 mg/kg for 2 consecutive days), and GVHD prophylaxis consisted of the combined use of cyclosporine A (CyA) and methylprednisolone (mPSL). HLA-DRB1 1-locus mismatched unrelated CB (2.08×10^7 total nucleated cells per kilogram) was transplanted on October 9, 1999 (10 days after the accident). Granulocyte colony-stimulating factor (G-CSF), erythropoietin, and thrombopoietin were concurrently administered to augment the hematopoietic recovery. The granulocyte count rose to more than 500/mm^3 on day 15 after CBT. Donor/recipient mixed chimerism was attained at engraftment, and it was confirmed by chromosomal analysis and fluorescence-labeled in situ hybridization technique (FISH) with Y-chromosome specific probes. We reduced the dose of CyA and mPSL gradually to avoid GVHD and undesirable opportunistic infection. Autologous hematopoietic recovery was completed by day 50 after CBT.

Transient reactivation of cytomegalovirus (CMV) was detected by CMV-antigenemia analysis with CMV-specific mouse monoclonal antibodies (C10 and C11) of patient-derived granulocytes and by CMV polymerase chain reaction (PCR) of patient-derived plasma. CMV infection was successfully treated by the administration of ganciclovir, because the patient's $CD8^+$ lymphocyte count increased concurrently [23]. Radiation burns of the face, throat, and extremities worsened in conjunction with autologous hematopoietic recovery. Allogeneic cadaver skin transplantation failed to restore the skin and mucocutaneous barriers; the result was colonization of methicillin-resistant *Staphylococcus aureus* on the patient's skin and throat despite concomitant administration of vancomycin with arbekacin. The patient suffered from obstructive sleep apnea syndrome, which was caused by a blood clot in the oral cavity. The patient died of aspiration pneumonia and ARDS 210 days after the accident.

Recovered autologous bone marrow contained complex chromosomal abnormalities [23], and immune function was investigated as described below. All materials examined were collected from the patient and used after signed informed consent according to the Declaration of Helsinki.

2.2. Flow Cytometry

Patient PB mononuclear cells (PBMNCs) were separated by density gradient with centrifuge and Ficoll-Hypaque (Pharmacia Biotech, Uppsala, Sweden), treated with 0.5% mouse serum (Dako, Glostrup, Denmark) for 15 minutes at 4°C to block nonspecific Fc receptor binding, and incubated with 1 or 2 of following monoclonal antibodies (MoAbs) conjugated to fluorescein isothiocyanate (FITC) or phyco-

International Journal of
HEMATOLOGY

Case Report

Severe Immune Dysfunction after Lethal Neutron Irradiation in a JCO Nuclear Facility Accident Victim

Hitomi Nagayama,[a,b] Jun Ooi,[a] Akira Tomonari,[a] Tohru Iseki,[a] Arinobu Tojo,[a] Kenzaburo Tani,[a] Tsuneo A. Takahashi,[a] Naohide Yamashita,[a] Shigetaka Asano[a]

[a]Institute of Medical Science, University of Tokyo; [b]Division of Hematology, Department of Medicine, Keio University School of Medicine, Tokyo, Japan

Received February 22, 2002; received in revised form April 25, 2002; accepted April 30, 2002

Abstract

The optimal treatment for the hematological toxicity of acute radiation syndrome (ARS) is not fully established, especially in cases of high-dose nonuniform irradiation by mixed neutrons and γ-rays, because estimation of the irradiation dose (dosimetry) and prediction of autologous hematological recovery are complicated. For the treatment of ARS, we performed HLA-DRB1–mismatched unrelated umbilical cord blood transplantation (CBT) for a nuclear accident victim who received 8 to 10 GyEq mixed neutron and γ-ray irradiation at the JCO Co. Ltd. nuclear processing facility in Tokaimura, Japan. Donor/recipient mixed chimerism was attained; thereafter rapid autologous hematopoietic recovery was achieved in concordance with the termination of immunosuppressants. Immune function examined in vitro showed recovery of the autologous immune system was severely impaired. Although the naive T-cell fraction and the helper T-cell subtype 1 fraction were increased, the mitogenic responses of T-cells and the allogeneic mixed leukocyte reaction were severely suppressed. Endogenous immunoglobulin production was also suppressed until 120 days after the accident. Although skin transplantation for ARS was successful, the patient died of infectious complications and subsequent acute respiratory distress syndrome 210 days after the accident. These results suggest that fast neutrons in doses higher than 8 to 10 Gy cause complete abrogation of the human immune system, which may lead to fatal outcome even if autologous hematopoiesis recovers. The roles of transplantation, autologous hematopoietic recovery, chimerism, immune suppression, and immune function are discussed. *Int J Hematol.* 2002;76:157-164.

Key words: Neutron irradiation; Umbilical cord blood transplantation; Autologous hematopoietic recovery; Immune dysfunction

1. Introduction

The feasibility and efficacy of allogeneic bone marrow transplantation (BMT) for accidentally irradiated individuals remains unclear because of the high incidence of mortality due to acute graft-versus-host disease (GVHD) and ensuing acute radiation syndrome (ARS) [1,2]. After the Chernobyl accident, 11 of 13 BMT recipients died of burns, gastrointestinal (GI) bleeding, interstitial pneumonitis, acute respiratory distress syndrome (ARDS), and GVHD. Experimentally transplanted fetal liver cells failed to engraft in the 7 adult recipients, because the transplants contained limited numbers of hematopoietic stem cells (HSCs). Only 2 long-term Chernobyl survivors who underwent BMT have been supported by autologous hematopoietic recovery [1]. Because of the high incidence of non–bone marrow toxicities and transplant-related mortality, the indications for HSC

Correspondence and reprint requests: Hitomi Nagayama, MD, PhD, Division of Hematology, Department of Medicine, Keio University School of Medicine, 35 Shinanomachi, Shinjuku-ku, Tokyo 160-8582, Japan; 81-3-5363-3785; fax: 81-3-3353-3515 (e-mail: zephyrus@sc.itc.keio.ac.jp).

References

1 Dranoff G, Jaffee E, Lazenry A *et al.* Vaccination with irradiated tumor cells engineered to secrete murine granulocyte-macrophage colony-stimulating factor stimulates potent, specific, and long-lasting anti-tumor immunity. *Proc. Natl Acad. Sci. USA* 1993; **90**: 3539–43.

2 Tani K, Nakazaki Y, Hase H *et al.* Progress reports on immune gene therapy for stage IV renal cell cancer using lethally irradiated granulocyte-macrophage colony-stimulating factor-transduced autologous renal cancer cells. *Cancer Chemother. Pharmacol.* 2000; **46** (Suppl.): S73–6.

3 Simons JW, Jaffee EM, Weber CE *et al.* Bioactivity of autologous irradiated renal cell carcinoma vaccines generated by ex vivo granulocyte-macrophage colony-stimulating factor gene transfer. *Cancer Res.* 1997; **57**: 1537–46.

4 Jaffee EM, Dranoff G, Cohen LK *et al.* High efficiency gene transfer into primary human tumor explants without cell selection. *Cancer Res.* 1993; **53** (Suppl. 10): 2221–6.

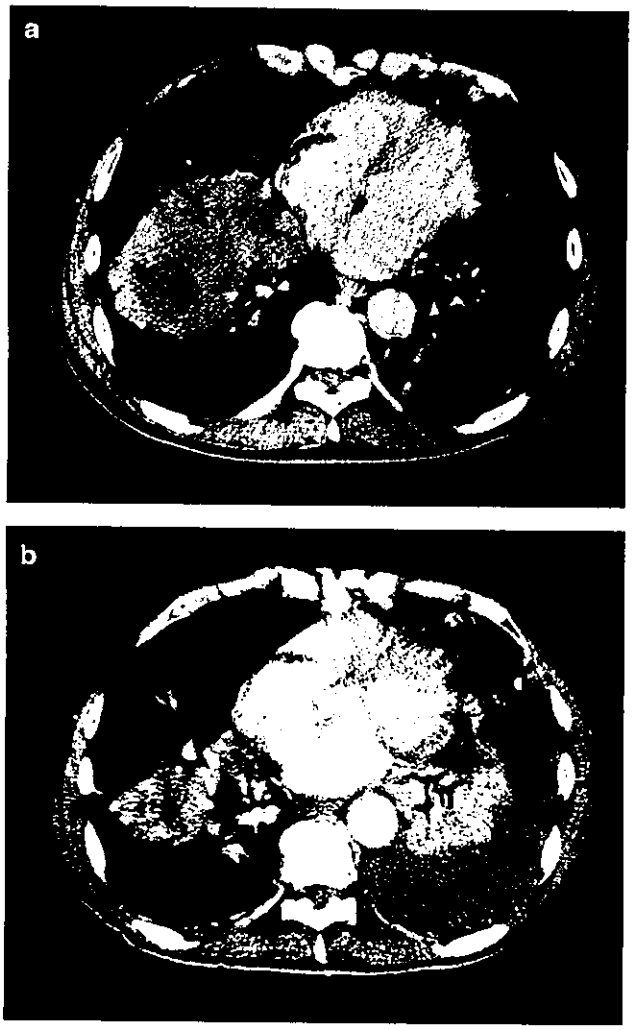

Fig. 3 Chest CT scan (a) before and (b) 1 month after the initiation of IL-2 treatment. Note the marked regression of a right lung hilar mass despite progression of the other metastatic nodules and pleural effusion.

any other changes associated with active autoimmune disease.

Discussion

Since RCC is thought to be an immunogenic cancer, gene immunotherapy is considered to be one of the challenging gene therapy strategies. In 1997, Simons *et al.* reported a phase I study of autologous RCC vaccination in the USA.[3] An objective partial response was observed in one of seven patients treated with GM-CSF gene-transduced tumor vaccine.[3] In Japan, a phase I study of a GM-CSF gene-transduced tumor vaccine for metastatic RCC patients (the first cancer gene therapy in the country) is currently being conducted as a multi-institutional study organized by IMSUT. The procedure for producing autologous vaccine cells is conducted at IMSUT under Good Manufacturing Practices. Although the treatment protocol is essentially the same as the one reported by Simons *et al.*,[3] the vaccination schedule is longer in the current study than in the previous clinical trial conducted in the USA.

The objectives of the current study are to test the safety of the gene therapy and evaluate immunological anti-tumor effects. In the present paper we reported the clinical course of the first patient enrolled in the study. During and after gene therapy, no remarkable side-effects were observed by physical examination or laboratory tests. In addition, no pathological findings specific to gene immunotherapy, such as autoimmune disease, were found by autopsy. To our knowledge, this is the first detailed report of an autopsy of a patient treated with GM-CSF gene therapy.

Despite the strong positive DTH conversion against autologous RCC cells after vaccination, the clinical response of the GM-CSF gene therapy resulted in progressive disease. However, the subsequent low-dose IL-2 therapy showed rapid and remarkable regression in a large lung hilar metastatic mass. The most striking histological finding in the responding mass was CD8 positive T-cell infiltration. It suggests the CD8 positive T-cell might be an important effector cell in regression of the mass. Since the mass regressed after IL-2 therapy, it is not certain that the GM-CSF gene therapy plays a role in this immune response. Further clinical and immunological evaluation of the other patients enrolled in the study is required.

Finally, there was a difference in RCC histology between the nephrectomised primary site and the metastatic sites. This may have been the result of natural selection of metastatic phenotype, because it is well known that metastases from clear cell at the primary site are not always clear cell and may be considerably less differentiated than cells at the primary site. Another possibility is the selective escape of non-clear cell populations from immunity induced by vaccine prepared from clear cell carcinoma, which was dominant at the primary site. Although it is not clear whether selective escape might be involved in the present case, the genetic instability and heterogeneous features of RCC may require additional treatment combined with immune gene therapy. At the time of this report, the trial is in progress, and an additional three patients have been successfully treated with no significant side-effects. Further clinical and immunological evaluation including these patients is required to ascertain the clinical benefits of GM-CSF gene therapy in metastatic RCC.

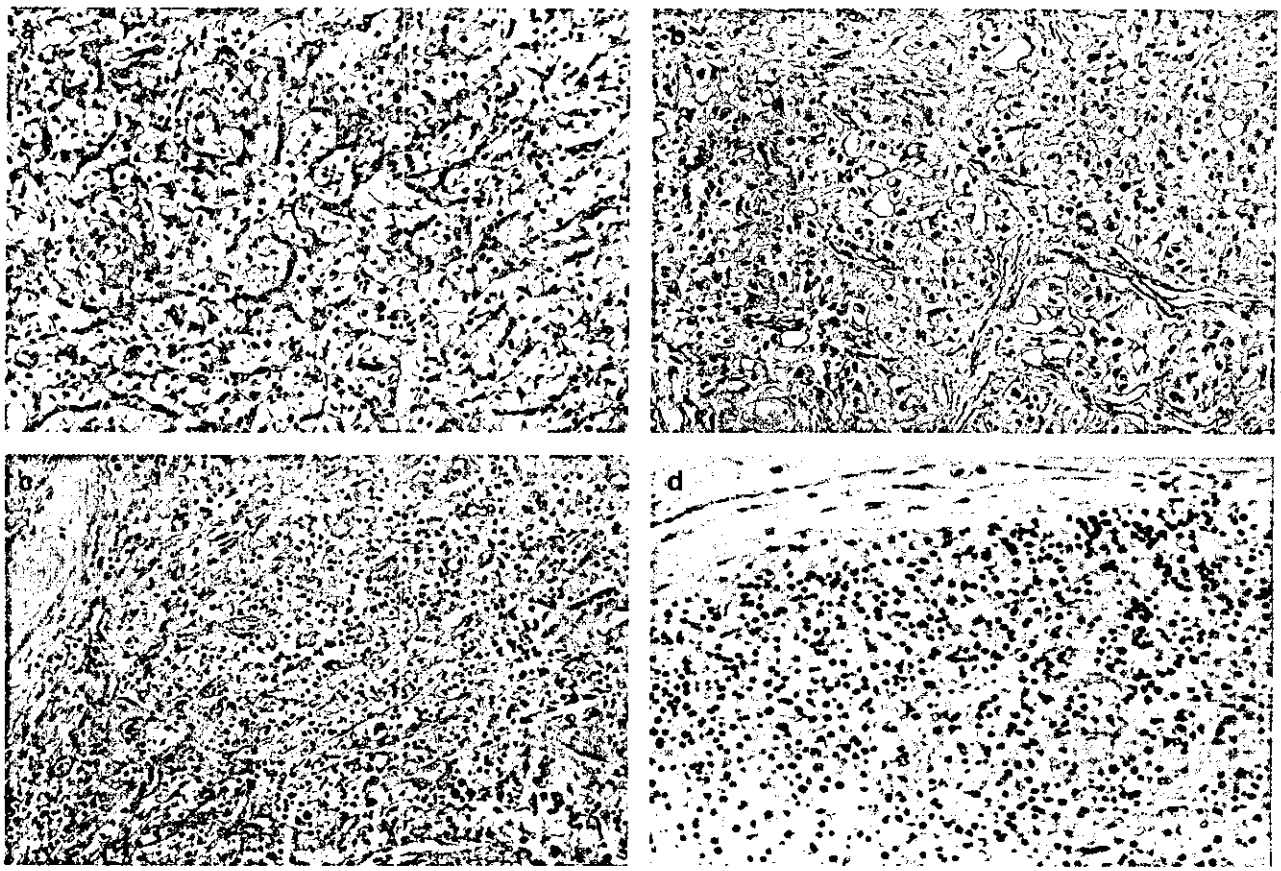

Fig. 2 H&E staining × 100 of the (a) nephrectomised primary lesion, (b) lung metastatic lesions and (c) right lung hilar metastasis. (d) Immunohistochemical staining with anti-CD8 antibody of the right hilar mass (× 100). The largest part of the primary site consisted of clear cell carcinoma (a), whereas most metastatic sites consisted of granular cell carcinoma (b). The right lung hilar metastasis (the nodule that responded after IL-2 therapy) showed diffuse necrotic change (c). Immunohistochemistry revealed CD8 positive T-lymphocyte dominant infiltration of the right lung hilar metastasis (d).

for a total IL-2 dose of 20×10^6 JRU. However, the patient's condition deteriorated due to progression of metastases. The patient died of multiple RCC metastases 9 months after nephrectomy and 7 months after the start of GM-CSF gene therapy.

Autopsy and histological findings

With permission from the family, an autopsy was performed 5 h after the patient's death. Grossly massive RCC metastases were found in both lungs and the liver. Widespread metastases were also found in the pancreas, duodenum, left kidney, pleura and retroperitoneal lymph nodes. Histological examination of the metastasis sites showed that almost all examined nodules consisted of granular cell carcinoma, which was in sharp contrast to the histology of the primary site where clear cell carcinoma was dominant (Figs 2a,b). In addition, sarcomatoid changes were observed in the kidney metastasis. These findings indicate the apparent histological divergence of metastatic sites. While scattered necrotic foci were seen, RCC cells were morphologically viable in most of the metastatic sites. In contrast, histology of the right lung hilar metastasis, the lesion that shrank after IL-2 therapy, showed diffuse necrotic changes (Fig. 2c). Viable cells were barely seen in pseudocapsule of this lesion as bizarre foci of granular cell carcinoma. No significant differences were found in the degree of lymphocyte infiltration and dendritic cell infiltration; however, the shrunk lesion was infiltrated with proportionately more CD8 positive T lymphocytes, compared to other non-responding metastatic lesions, as shown in Fig. 2d. The similar CD8 positive T-lymphocyte accumulation was seen in one necrotic deposit in the liver. Careful histological examination did not reveal vasculitis or

Fig. 1 Plain chest X-ray showing a large metastatic mass in the right hilar region and multiple metastases in both lungs.

Case report

Clinical course

A 60-year-old man with gross hematuria was seen at Tsukuba University Hospital (TUH) in September 1998. The patient was diagnosed as stage IV RCC (UICC classification 1997) with multiple lung metastases (Fig. 1). Following careful screening for eligibility criteria and after providing written informed consent, the patient was transferred to the Research Hospital of IMSUT, where he was enrolled in a phase I study of GM-CSF gene therapy. A 10 cm RCC tumor arising from the upper pole of the right kidney was resected, and the cell processing began on the same day. The largest part of resected tumor consisted of clear cell carcinoma with nuclear grade 2 as shown in Fig. 2a. The autologous RCC cell culture from 80 g of tumor tissue was successfully propagated, and the human GM-CSF gene was introduced using the MFG-S retrovirus vector.[1–4] Four-hundred and sixty million transduced cells with GM-CSF production of 49 ng/10^6 cells per 24 h were harvested. The harvested vaccine cells were lethally irradiated with 150 Gy of X-ray, then frozen in aliquots and stored in liquid nitrogen. BioReliance (Rockville, Maryland, USA) conducted standard safety testing according to US Food and Drug Administration guidelines and confirmed that culture supernatants were free of replication-competent retrovirus (RCR).

After safety and release testing, GM-CSF gene therapy was initiated by subcutaneous injection of vaccine cells. From December 1998 to April 1999, the patient was injected with a total of 2.2×10^8 vaccine cells divided into ten doses (4×10^7 cells in the first injection, followed by 2×10^7 cells at 2-week intervals). The patient experienced no remarkable side-effects except for low-grade fever, and local erythema and induration at the vaccination sites, both of which resolved spontaneously. Laboratory tests revealed no remarkable changes except transient eosinophilia up to 700 cells/mm^3, which peaked 48 h after vaccination and returned to normal the next day. There was no significant alteration in the serum GM-CSF level after vaccination. During the course of vaccination, the delayed-type hypersensitivity (DTH) reaction was examined by the intradermal injection of 1×10^6 lethally irradiated cultured autologous RCC cells (non-transduced RCC cells) as an in-vivo immunological examination.[3] As a control, the same number of lethally irradiated cultured autologous normal kidney cells, which were prepared from normal part of nephrectomy tissue, were injected intradermally. Reactions to DTH increased markedly after the start of vaccination; however, weak reaction was also observed at the site of normal kidney cell injection.

After therapy began, the growth of the largest lung hilar mass, as evaluated by helical computed tomography (CT), had slowed to some extent; however, new multiple nodules appeared in other lung fields. The patient maintained good performance status until the 10th injection, but routine radiographic examination at that time revealed development of new metastases in the liver and brain. At this point, vaccination was discontinued, and the patient was transferred to TUH for further treatment and supportive care. No RCR was detected in blood samples during or after the end of vaccination.

After transfer to TUH, asymptomatic brain metastases were treated with a single session of gamma-knife radiosurgery for prevention of central nervous system complications. Intravenous administration of human recombinant interleukin (IL)-2 (Teceleukin, Shionogi, Osaka), at a daily dose of $0.7–1.4\times10^6$ Japan Reference Unit (JRU), began 1 month after the end of the vaccination period. A few weeks after the start of IL-2 therapy, chest X-ray revealed a decrease in the size of the right hilar large mass, despite new metastatic deposits and pleural effusion in both lungs. The findings were confirmed by chest CT scan 1 month after the start of IL-2 therapy (Fig. 3). Treatment continued for 5 weeks

International Journal of Urology (2002) **9**, 462–466

Case Report

Advanced renal cell carcinoma treated with granulocyte-macrophage colony-stimulating factor gene therapy: A clinical course of the first Japanese experience

KOJI KAWAI,[1] KENZABURO TANI,[2] NAOHIDE YAMASHITA,[2] SHINJI TOMIKAWA,[2] MASAZUMI ERIGUCHI,[2] MAKOTO FUJIME,[3] KO OKUMURA,[3] TADAO KAKIZOE,[4] SHIRLEY CLIFT,[5] DALE ANDO,[5] RICHARD MULLIGAN,[6] ATSUSI YAMAUCHI,[1] MASAYUKI NOGUCHI,[7] SHIGETAKA ASANO[2] AND HIDEYUKI AKAZA[1]

Departments of [1]Urology and [7]Pathology, Institute of Clinical Medicine, University of Tsukuba, Ibaraki, [2]Advanced Clinical Research Center, Institute of Medical Science, University of Tokyo, [3]Department of Urology, School of Medicine, Jutendo University, [4]Urology Division, National Cancer Center Hospital, Tokyo, Japan, [5]Cell Genesys, Foster City, California and [6]School of Medicine, Harvard University, Boston, Massachusetts, USA

Abstract A phase I study of granulocyte-macrophage colony-stimulating factor (GM-CSF) gene-transduced tumor vaccine for patients with metastatic renal cell carcinoma (RCC) was initiated in 1998, as the first cancer gene therapy in Japan. The study is still ongoing, but the first patient is presented here as a case report. The patient was a 60-year-old man with Stage IV CRC with multiple lung metastases. After surgical resection of the tumor, autologous tumor cells were transduced and cultured to produce GM-CSF. The patient received a total of 2.2×10^8 gene-transduced autologous vaccine cells by subcutaneous injection. During the course of vaccination, growth of the largest metastatic mass slowed to some extent; however, multiple new lesions developed. About 1 month after the start of low-dose IL-2 therapy, rapid and remarkable regression in a large lung hilar metastatic mass was noticed. The patient died of progressive disease 7 months after the start of GM-CSF gene therapy. Careful histological examination by autopsy revealed that the responding mass was infiltrated by CD8 positive dominant T lymphocytes, and did not exhibit vasculitis or any other changes associated with active autoimmune disease.

Key words gene therapy, granulocyte-macrophage colony-stimulating factor, renal cell carcinoma, vaccine.

Introduction

Treatment options for metastatic renal cell carcinoma (RCC) are limited due to the lack of effective systemic therapy. According to preclinical animal studies, vaccination using autologous granulocyte-macrophage colony-stimulating factor (GM-CSF) transduced tumor cells is considered to be one of the challenging immunotherapies for RCC.[1] In April 1998, we submitted our preclinical data on cell processing and gene transfer to the Institute of Medical Science, University of Tokyo (IMSUT) Institutional Review Board. In August 1998, the Japanese government granted permission to initiate gene therapy. Within the same year, the phase I study of a GM-CSF gene-transduced tumor vaccine for patients with metastatic RCC began as the first cancer gene therapy in Japan.[2] The study is currently being conducted as a multi-institutional study organized by IMSUT. The present report describes the clinical course of the first patient who received the GM-CSF gene therapy.

Correspondence: Koji Kawai MD, Department of Urology, Institute of Clinical Medicine, University of Tsukuba, 1-1-1 Tennodai, Tsukuba-city, Ibaraki 305, Japan.
Email: rkawa@md.tsukuba.ac.jp
Received 16 August 2001; accepted 28 February 2002.

18. Sato, K., H. Nagayama, and T. A. Takahashi. 1999. Aberrant CD3- and CD28-mediated signaling events in cord blood T cells are associated with dysfunctional regulation of Fas ligand-mediated cytotoxicity. *J. Immunol. 162:4464.*
19. Sato, K., H. Kawasaki, H. Nagayama, M. Enomoto, C. Morimoto, K. Tadokoro, T. Juji, and T. A. Takahashi. 2000. TGF-β1 reciprocally controls chemotaxis of human peripheral blood monocyte-derived dendritic cells via chemokine receptors. *J. Immunol. 164:2285.*
20. Ayehunie, S., E. A. Garcia-Zepeda, J. A. Hoxie, R. Horuk, T. S. Kupper, A. D. Luster, and R. M. Ruprecht. 1997. Human immunodeficiency virus-1 entry into purified blood dendritic cells through CC and CXC chemokine receptors. *Blood 90:1379.*
21. Funda, D. P., L. Tuckova, M. A. Farre, T. Iwase, I. Moro, and H. Tlaskalova-Hogenova. 2001. CD14 is expressed and released as soluble CD14 by human intestinal epithelial cells in vitro: lipopolysaccharide activation of epithelial cells revisited. *Infect. Immun. 69:3772.*
22. Combadiere, C., S. K. Ahuja, H. L. Tiffany, and P. M. Murphy. 1996. Cloning and functional expression of CC CKR5, a human monocyte CC chemokine receptor selective for MIP-1α, MIP-1β, and RANTES. *J. Leukocyte Biol. 60:147.*
23. Neote, K., D. DiGregorio, J. Y. Mak, R. Horuk, and T. J. Schall. 1993. Molecular cloning, functional expression and signaling characteristics of a C-C chemokine receptor. *Cell 72:415.*
24. Nardelli, B., H. L. Tiffany, G. W. Bong, P. A. Yourey, D. K. Morahan, Y. Li, P. M. Murphy, and R. F. Alderson. 1999. Characterization of the signal transduction pathway activated in human monocytes and dendritic cells by MPIF-1, a specific ligand for CC chemokine receptor 1. *J. Immunol. 162:435.*
25. Al-Aoukaty, A., B. Rolstad, A. Giaid, and A. A. Maghazachi. 1998. MIP-3α, MIP-3β and fractalkine induce the locomotion and the mobilization of intracellular calcium, and activate the heterotrimeric G proteins in human natural killer cells. *Immunology 95:618.*
26. Biesen, T. V., B. E. Hawea, D. K. Luttrell, K. M. Krueger, K. Touhara, E. Porfiri, M. Sakaue, L. M. Luttrell, and R. J. Lefkowitz. 1995. Receptor-tyrosine-kinase- and G$\beta\gamma$-mediated MAP kinase activation by a common signaling pathway. *Nature 376:781.*
27. Dikic, I., G. Tokiwa, S. Lev, S. A. Courteidge, and J. Schlessinger. 1996. A role for Pyk2 and Src in linking G-protein-coupled receptors with MAP kinase activation. *Nature 383:547.*
28. Bacon, K. B., M. C. Szabo, H. Yssel, J. B. Bolen, and T. J. Schall. 1996. RANTES induces tyrosine kinase activity of stably complexed p125^{FAK} and ZAP-70 in human T cells. *J. Exp. Med. 184:873.*
29. Davis, C. B., I. Dikic, D. Unutmaz, C. M. Hill, J. Arrthos, M. A. Siani, D. A. Thompson, J. Schlessinger, and D. R. Littman. 1997. Signal transduction due to HIV-1 envelope interactions with chemokine receptors CXCR4 or CCR5. *J. Exp. Med. 186:1793.*
30. Ganju, R. K., P. Dutt, L. Wu, W. Newman, H. Avraham, S. Avraham, and J. E. Groopman. 1998. β-chemokine receptor CCR5 signals via novel tyrosine kinase RAFTK. *Blood 91:791.*
31. Coso, O. A., H. Teramoto, W. F. Simonds, and J. S. Gutkind. 1996. Signaling from G protein-coupled receptors to c-Jun kinase involves $\beta\gamma$ subunits of heterotrimeric G proteins acting on a Ras and Rac1-dependent pathway. *J. Biol. Chem. 271:3963.*
32. Neer, E. J. 1995. Heterotrimeric G proteins: organizer of transmembrane signals. *Cell 80:249.*
33. Al-Aoukaty, A., T. J. Schall, and A. A. Maghazachi. 1996. Differential coupling CC chemokine receptors to multiple heterotrimeric G proteins in human interleukin-2-activated natural killer cells. *Blood 87:4255.*
34. Arai, H., and I. F. Charo. 1996. Differential regulation of G-protein-mediated signaling by chemokine receptors. *J. Biol. Chem. 271:21814.*
35. Sotsios, Y., G. C. Whittaker, J. Westwick, and S. G. Ward. 1999. The CXC chemokine stromal cell-derived factor activates a G_i-coupled phosphoinositide 3-kinase in T lymphocytes. *J. Immunol. 163:5954.*
36. Kehrl, J. H. 1998. Heterotrimeric G protein signaling: roles in immune function and fine-tuning by RGS proteins. *Immunity 8:1.*
37. Bowman, E. P., J. J. Campbell, K. M. Druey, A. Scheschonka, J. H. Kehrl, and E. C. Butcher. 1998. Regulation of chemotactic and proadhesive responses to chemoattractant receptors by RGS (regulator of G-protein signaling) family members. *J. Biol. Chem. 273:28040.*
38. Moratz, C., V. H. Kang, K. M. Druey, C.-S. Shi, A. Scheschonka, P. M. Murphy, T. Kozasa, and J. H. Kehrl. 2000. Regulator of G protein signaling 1 (RGS) markedly impairs $G_{i\alpha}$ signaling responses of B lymphocytes. *J. Immunol. 164: 1829.*
39. Yan, Y., P. P. Chi, and H. R. Bourne. 1997. RGS4 inhibited Gq-mediated activation of mitogen-activated protein kinase and phosphoinositide synthesis. *J. Biol. Chem. 272:11924.*
40. Reif, K., and J. G. Cyster. 2000. RGS molecule expression in murine B lymphocytes and ability to down-regulate chemotaxis to lymphoid chemokines. *J. Immunol. 64:4720.*
41. Rose, P. M., S. R. J. Krystek, P. S. Patel, E. C. Liu, J. S. Lynch, D. A. Lach, S. M. Fisher, and M. L. Webb. 1995. Aspartate mutation distinguishes ETA but not ETB receptor subtype-selective ligand binding while abolishing phospholipase C activation in both receptors. *FEBS Lett. 361:243.*
42. Parent, J. L., C. Le Gouill, M. Rola-Pleszczynski, and J. Stankova. 1996. Mutation of an aspartate at position 63 in the human platelet-activating factor receptor augments binding affinity but abolishes G-protein-coupling and inositol phosphate production. *Biochem. Biophys. Res. Commun. 219:968.*
43. D'Amico, G., G. Frascaroli, G. Bianchi, P. Transidico, A. Doni, A. Vecchi, S. Sozzani, P. Allavena, and A. Mantovani. 2001. Uncoupling of inflammatory chemokine receptors by IL-10: generation of functional decoys. *Nat. Immunol. 1:387.*
44. Murai, M., H. Yoneyama, A. Harada, Z. Yi, C. Vestergaard, B. Guo, K. Suzuki, H. Asakura, and K. Matsushima. 1999. Active participation of CCR5$^+$CD8$^+$ T lymphocytes in the pathogenesis of liver injury in graft-versus-host disease. *J. Clin. Invest. 104:49.*

because CCR1 is the only receptor for CCL3 and CCL5 in this subset.

Uncoupling of GPCRs with G proteins is thought to prevent their high-affinity ligand binding (24). We showed that pretreatment of the cell membrane fractions obtained from memory and naive $CD4^+$ T cells with GTP-γS inhibited their ligand binding. Therefore, the high-affinity ligand binding of CCR1 and/or CCR5 in both cell types may involve their coupling with G proteins. In contrast, CCL5 induced GTP-GDP exchange in memory $CD4^+$ T cells, whereas this stimulation failed to induce this event in naive $CD4^+$ T cells. These phenomena imply that the ligation of CCR1 by CCL5 may not induce GTP-GDP exchange in $G_{i\alpha}$ and $G_{q\alpha}$ in naive $CD4^+$ T cells, although these G protein subunits may bind the CCL5-CCR1 complex. In contrast, mutation of GPCRs and certain stimulations led to the retention of a high ligand binding affinity of GPCRs but abolished their downstream signaling events, although the precise mechanism remains unclear (41–43). Therefore, our findings involving GTP-GDP exchange in G_α subunits and the ligand binding affinity of CCR1 in naive $CD4^+$ T cells may be a novel regulatory mechanism for GPCR. Collectively, our findings suggest that a failure of CCR1 to activate PTK-dependent cascade may involve the deficiency in the ligand-induced GTP-GDP exchange in $G_{i\alpha}$ and $G_{q\alpha}$.

The intracellular expressions of RGS3 and RGS4 were only detected in naive $CD4^+$ T cells. It has been previously reported that the expression of RGS1, RGS3, and RGS4, but not RGS2, suppressed the chemotactic response of certain transfectants to FMLP, C5a, CXCL8/IL-8, and CCL2/monocyte chemoattractant protein-1, while the expression of RGS3 and RGS4 inhibited the CCL3-induced CCR1-mediated chemotaxis of these cell types (37). In contrast, $p60^{Src}$ and Pyk2 link GPCR with various downstream PTK-dependent cascades (26, 27, 30, 31). In addition, Yan et al (39) have previously reported that RGS4 inhibited $G_{q\alpha}$-mediated activation of MAPKs in certain transfectants. However, the role of RGS3 and RGS4 in the defective CCL5-induced CCR1-mediated signaling events in naive $CD4^+$ T cells remains unknown because RGS proteins are not thought to affect GTP-GDP exchange (36–39); the failure of ligand-induced GTP-GDP exchange in G_α subunits may play a crucial role in these events. These phenomena imply that RGS3 and RGS4 would not contribute to the failure of CCR1 to activate G_α subunit-dependent signaling events in naïve $CD4^+$ T cells.

Naive $CD4^+$ T cells showed greater surface expression level of CXCR4 and response to CXCL12 than memory $CD4^+$ T cells. In addition, CXCL12-induced GTP binding to $G_{i\alpha}$ in naive $CD4^+$ T cells was higher than in memory $CD4^+$ T cells. Moratz et al. (38) have previously reported that the impairment of CXCL12-induced CXCR4-mediated migratory responsiveness in germinal center B cells involved a constitutive expression of RGS1, whereas CXCL12 attracted CXCR4-expressed naive and memory B cells lacking the expression of RGS1. We showed that memory $CD4^+$ T cells as well as naive $CD4^+$ T cells did not exhibit the intracellular expression of RGS1. Therefore, the difference in the response to CXCL12 between memory and naive $CD4^+$ T cells may be correlated with the cell surface expression level of CXCR4- and CXCL12-induced GTP-GDP exchange in $G_{i\alpha}$. However, Reif et al. (40) have recently reported that a short isoform of RGS3 (sRGS3) as well as RGS1 are effective inhibitors of $G_{i\alpha}$-dependent response to CXCL12 in murine B cell transfectants. The discrepancy in the role of RGS3 between human $CD4^+$ T cells and the murine B cell line in the CXCL12-induced response via CXCR4 remains unclear; this might be due to the isoform variances or the species differences.

In summary, our findings suggest that the failure of ligand-induced activation of CCR1-mediated downstream signaling events as well as the deficiency of CCR5 expression are associated with the hyporesponsiveness of human naive $CD4^+$ T cells to CCL3 and CCL5. We (16) and others (9) have previously reported that CCR2, CCR6, and CXCR3 were only expressed on memory $CD4^+$ T cells, and their expression patterns were associated with the respective chemokine responsiveness. Thus, the different chemotactic properties of memory and naive $CD4^+$ T cells may be explained by chemokine receptor expression levels as well as their abilities to activate downstream signaling events. Aberrant trafficking properties of T cells are suggested to be involved in the initiation and persistence of immunopathological diseases (1–3, 44). Furthermore, chemokines and their receptor system are thought to be potential target molecules for therapeutic intervention to prevent these diseases (1–3, 44). Thus, the molecular manipulation of chemokine receptor-mediated signaling events may be a novel approach to the prevention and therapy of immunopathological diseases.

Acknowledgments

We thank M. Yamamoto for excellent assistance.

References

1. Rollins, B. J. 1997. Chemokines. *Blood 90:909.*
2. Ward, S. G., K. Bacon, and J. Westwick. 1998. Chemokines and T lymphocytes: more than an attraction. *Immunity 9:1.*
3. Zlotnik, A. and O. Yoshie. 2000. Chemokines: a new classification system and their role in immunity. *Immunity 12:121.*
4. Loetscher, P., M. Seitz, M. Baggiolini, and B. Moser. 1996. Interleukin-2 regulates CC chemokine receptor expression and chemotactic responsiveness in T lymphocytes. *J. Exp. Med. 184:569.*
5. Schall, T. J., K. Bacon, K. J. Toy, and D. V. Goeddel. 1990. Selective attraction of monocytes and T lymphocytes of the memory phenotype by cytokine RANTES. *Nature 347:669.*
6. Schall, T. J., K. Bacon, R. D. R. Camp, J. W. Kaspari, and D. V. Goeddel. 1993. Human macrophage inflammatory protein α (MIP-1α) and MIP-1β chemokines attract distinct population of lymphocytes. *J. Exp. Med. 177:1821.*
7. Taub, D. D., K. Conlon, A. R. Lloyd, J. J. Oppenheim, and D. J. Kelvin. 1993. Preferential migration of activated $CD4^+$ and $CD8^+$ T cells in response to MIP-1α and MIP-1β. *Science 260:355.*
8. Qin, S., J. B. Rottman, P. Myers, N. Kassam, M. Weinblatt, M. Loetscher, A. E. Koch, B. Moser, and C. R. Mackay. 1998. The chemokine receptors CXCR3 and CCR5 mark subsets of T cells associated with certain inflammatory reactions. *J. Clin. Invest. 101:746.*
9. Rabin, R. L., M. K. Park, F. Liao, R. Swofford, D. Stephany, and J. M. Farber. 1999. Chemokine receptor responses on T cells are achieved through regulation of both receptor expression and signaling. *J. Immunol. 162:3840.*
10. Sallusto, F., D. Lenig, R. Forster, M. Lipp, and A. Lanzavecchia. 1999. Two subsets of memory T lymphocytes with distinct homing potentials and effector functions. *Nature 401:708.*
11. Liao, F., R. L. Rabin, C. S. Smith, G. Sharma, T. B. Nutman, and J. M. Farber. 1999. CC-chemokine receptor 6 is expressed on diverse memory subsets of T cells and determines responsiveness to macrophage inflammatory protein 3α. *J. Immunol. 162:186.*
12. Sallusto, F., C. R. Mackay, and A. Lanzavecchia. 1997. Selective expression of the eotaxin receptor CCR3 by human T helper 2 cells. *Science 277:2005.*
13. Bonecchi, R., G. Bianchi, P. P. Bordignon, D. Dambrosio, R. Lang, A. Borsatti, S. Sozzani, P. Allavena, P. A. Gray, A. Mantovani, and F. Sinigaglia. 1998. Differential expression of chemokine receptors and chemotactic responsiveness of type 1 T helper cells (Th1s) and Th2s. *J. Exp. Med. 187:129.*
14. Sallusto, F., D. Lenig, C. R. Mackay, and A. Lanzavecchia. 1998. Flexible programs of chemokine receptor expression on human polarized T helper 1 and 2 lymphocytes. *J. Exp. Med. 187:875.*
15. Imai, T., M. Nagira, S. Takagi, M. Kakizaki, M. Nishimura, J. Wang, P. W. Gray, K. Matsushima, and O. Yoshie. 1999. Selective recruitment of CCR4-bearing Th2 cells toward antigen-presenting cells by the CC chemokines thymus and activation-regulated chemokine and macrophage-derived chemokine. *Int. Immunol. 11:81.*
16. Sato, K., H. Kawasaki, H. Nagayama, M. Enomoto, C. Morimoto, K. Tadokoro, T. Juji, and T. A. Takahashi. 2001. Chemokine receptor expressions and responsiveness of cord blood T cells. *J. Immunol. 166:1659.*
17. Sato, K., H. Kawasaki, H. Nagayama, R. Serizawa, J. Ikeda, C. Morimoto, K. Yasunaga, N. Yamaji, K. Tadokoro, T. Juji, and T. A. Takahashi. 1999. CC chemokine receptors, CCR-1 and CCR-3, are potentially involved in antigen-presenting cell function of human peripheral blood monocyte-derived dendritic cells. *Blood 93:34.*

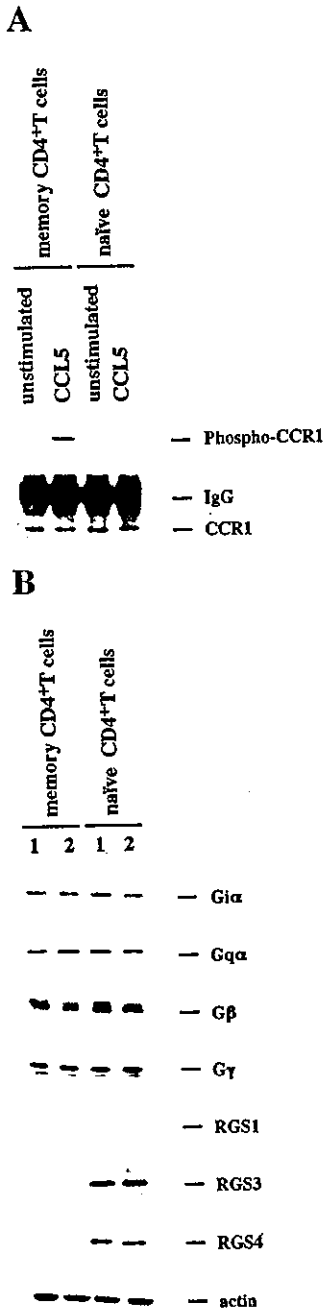

FIGURE 6. Expressions of $G_{\alpha\beta\gamma}$ complex and RGS proteins in memory and naive $CD4^+$ T cells. *A*, Memory and naive $CD4^+$ T cells were unstimulated or stimulated with CCL5. Immunoprecipitates obtained with Ab to CCR1 were analyzed by Western blotting with anti-pTyr mAb (phosphoproteins) and CCR1 to ensure that similar amounts of protein were present in each sample. *B*, Intracellular expression levels of G_α, G_β, G_γ, and RGS proteins in memory and naive $CD4^+$ T cells of two individuals were analyzed by Western blotting with the stated Abs. The results of Western blotting for actin demonstrate the loading of equal amounts of samples. The results are representative of 10 experiments.

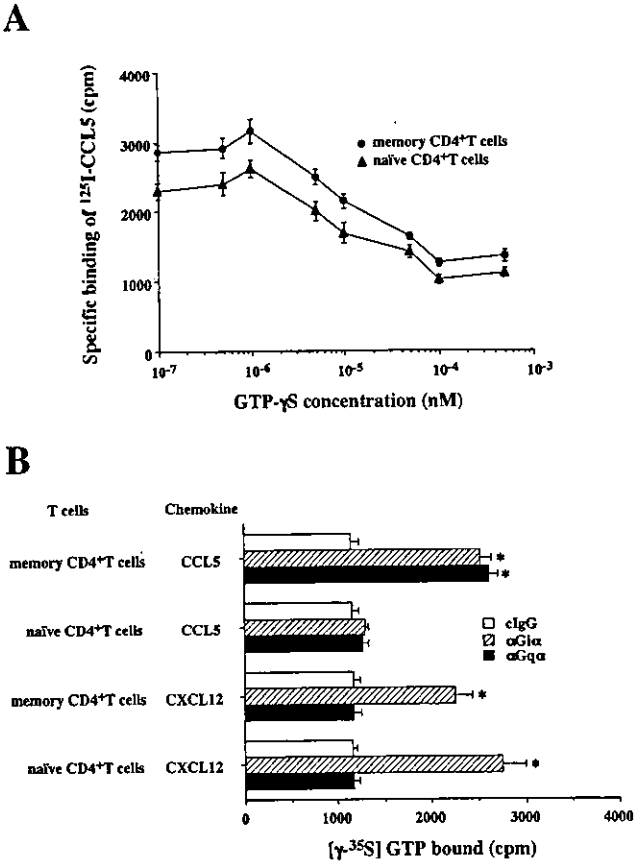

FIGURE 7. Effect of CCL5 binding on GTP-GDP exchange in memory and naive $CD4^+$ T cells. *A*, Effect of GTP-γS on the binding of ^{125}I-labeled CCL5 to cell membrane fractions was determined by preincubating cell membrane fractions with the indicated concentrations of GTP-γS (10^{-7}–10^{-3} nM) followed by incubation with ^{125}I-labeled CCL5 (~0.1 nM) in the presence of an excess of unlabeled CCL5 (10 nM). *B*, Cell membrane fractions obtained from memory and naive $CD4^+$ T cells were stimulated with CCL5 or CXCL12 and assayed for their GTP-GDP exchange. *, Value of $p < 0.001$ (compared with cIgG-activated cell membrane by Student's paired *t* test). The results are representative of 10 experiments.

and ligand binding, indicates that CCR1 and CCR5 play a role in these events ~80 and 20% of the time, respectively. Indeed, CCL3 and CCL5 exhibit more potent binding affinities to CCR1 than CCR5 by ~20-fold (22). Collectively, the deficiency of CCR5 expression is not the main reason for the hyporesponsiveness of naive $CD4^+$ T cells to CCL3 and CCL5. Thus, our results suggest that some other molecular mechanism involving CCR1-mediated signaling event accounts for the inability of naive $CD4^+$ T cells to respond to these inflammatory CCLs.

Stimulation with CCL5, CXCL12, or a combination of mAbs to CD3 and CD28 induced distinct patterns of tyrosine phosphorylation of intracellular proteins in total T cells and memory $CD4^+$ T cells, suggesting that specific PTK-dependent cascades are activated via the respective receptors, although several components may be shared. In contrast, the blocking experiments with mAbs to CCR1 and CCR5 show that CCR1 and CCR5 caused the different patterns and degree of tyrosine phosphorylation events in total T cells following stimulation with CCL5. Therefore, the ligation of CCR1 and CCR5 may activate the respective specific PTK-dependent cascade, although the precise difference in their downstream signaling event is still unclear because CCR1 and CCR5 share the ligands in total T cells and memory $CD4^+$ T cells (1–3).

We showed that the ligation by CCL5 activated CCR1- and CCR5-mediated PTK-dependent cascades in memory $CD4^+$ T cells, whereas this stimulation failed to induce these CCR1-mediated signaling events in naive $CD4^+$ T cells. In contrast, stimulation with CXCL12 via CXCR4 or mAbs to CD3 and CD28 caused marked tyrosine phosphorylation events in both cell types. These results suggest that the early section of CCR1-mediated PTK-dependent cascade is specifically repressed in naive $CD4^+$ T cells

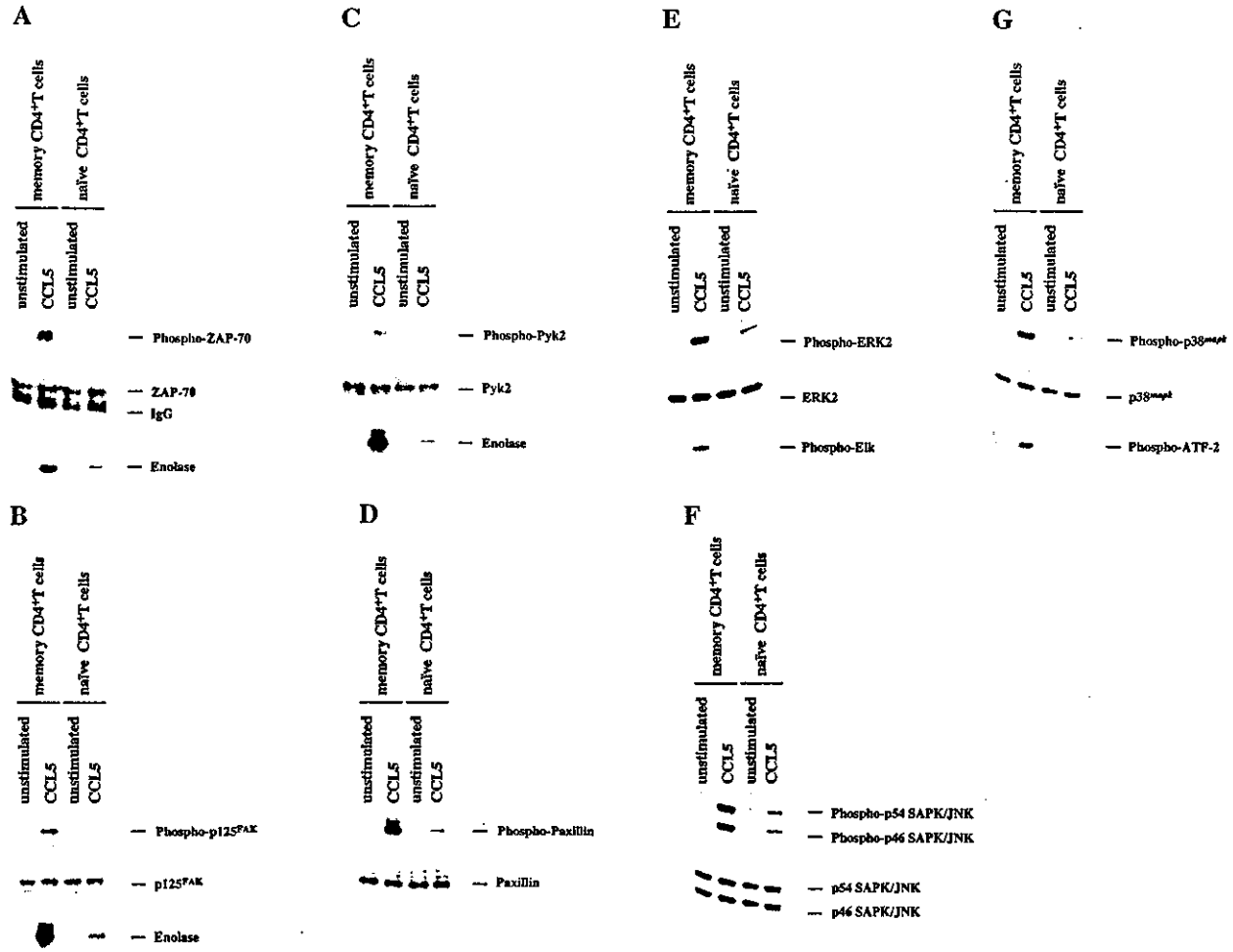

FIGURE 5. CCL5 activates PTKs and MAPKs in memory but not naive CD4$^+$ T cells. Memory and naive CD4$^+$ T cells were unstimulated or stimulated with CCL5. *A–D*, Immunoprecipitates obtained with Abs to ZAP-70 (*A*), p125^{FAK} (*B*), Pyk2 (*C*), and paxillin (*D*) were analyzed by Western blotting with anti-pTyr mAb (phosphoproteins) or the stated Abs to ensure that similar amounts of protein were present in each sample. *A–C*, In parallel experiments, immunoprecipitates obtained with the indicated Abs were assayed for their kinase activity with enolase as a substrate. *E–G*, Total cell lysates were analyzed by Western blotting with mAbs to ERK2 (*E*), SAPK/JNK (*F*), p38^{mapk} (*G*) or their tyrosine phosphorylated forms (*E–G*). In parallel experiments, immunoprecipitates obtained with anti-tyrosine phosphorylated ERK2 (*E*), c-*jun* fusion protein (*F*), or anti-tyrosine phosphorylated p38^{mapk} (*G*) were assayed for their kinase activities with Elk-1 (*E*), c-*jun* fusion protein (*F*), or ATF-2 (*G*) as a substrate. The results are representative of 10 experiments.

regulation of GPCR-mediated signaling events (36–39). Furthermore, accumulating results indicate that a family of RGS proteins were involved in the impairment of ligand-induced chemotaxis in certain cell types (37–40). Therefore, we examined the intracellular expression levels of RGS1, RGS3, and RGS4 in memory and naive CD4$^+$ T cells. Fig. 6*B* shows that RGS3 and RGS4 were only expressed in naive CD4$^+$ T cells, whereas RGS1 was undetected in either cell type.

Effect of CCL5 binding on GTP-GDP exchange in memory and naive CD4$^+$ T cells

To address the involvement of G proteins in the binding of CCL5 to memory and naive CD4$^+$ T cells, we examined the effect of GTP-γS on the binding of ^{125}I-labeled CCL5 to cell membrane fractions (Fig. 7*A*). Preincubation with GTP-γS suppressed the binding of ^{125}I-labeled CCL5 to the cell membrane fractions obtained from memory and naive CD4$^+$ T cells in a dose-dependent manner. These results indicate that CCR1- and/or CCR5-associated G proteins regulate the binding of CCL5 to memory and naive CD4$^+$ T cells.

We also examined the effect of CCL5 or CXCL12 on GTP-GDP exchange in cell membrane fractions obtained from memory and naive CD4$^+$ T cells (Fig. 7*B*). CCL5 enhanced the GTP binding to $G_{i\alpha}$ and $G_{q\alpha}$ in memory CD4$^+$ T cells, whereas this stimulation failed to induce this event in naive CD4$^+$ T cells. In contrast, CXCL12 enhanced the GTP binding to $G_{i\alpha}$, but not $G_{q\alpha}$, in both cell types.

Discussion

The findings reported in this work suggest that the hyporesponsiveness of naive CD4$^+$ T cells to CCL3 and CCL5 involves a failure of ligand-induced activation of CCR1-mediated downstream signaling event as well as a deficiency of CCR5 expression.

There are conflicting reports about the expression of CCR1 in PB naive CD4$^+$ T cells (9, 10, 16), although similar results for the chemotaxis of these subsets to CCL3 and CCL5 were obtained. Consistent with previous reports (9, 16), a similar expression level of CCR1 was observed in PB memory and naive CD4$^+$ T cells. In contrast, unlike PB naive T cells, cord blood naive CD4$^+$ T cells did not express CCR1 (16). This discrepancy might be due to the cell preparation and the binding affinity of anti-CCR1 mAb used in the experiments.

Analysis of the responsiveness of memory CD4$^+$ T cells to CCL5, with respect to cell surface expression levels, chemotaxis,

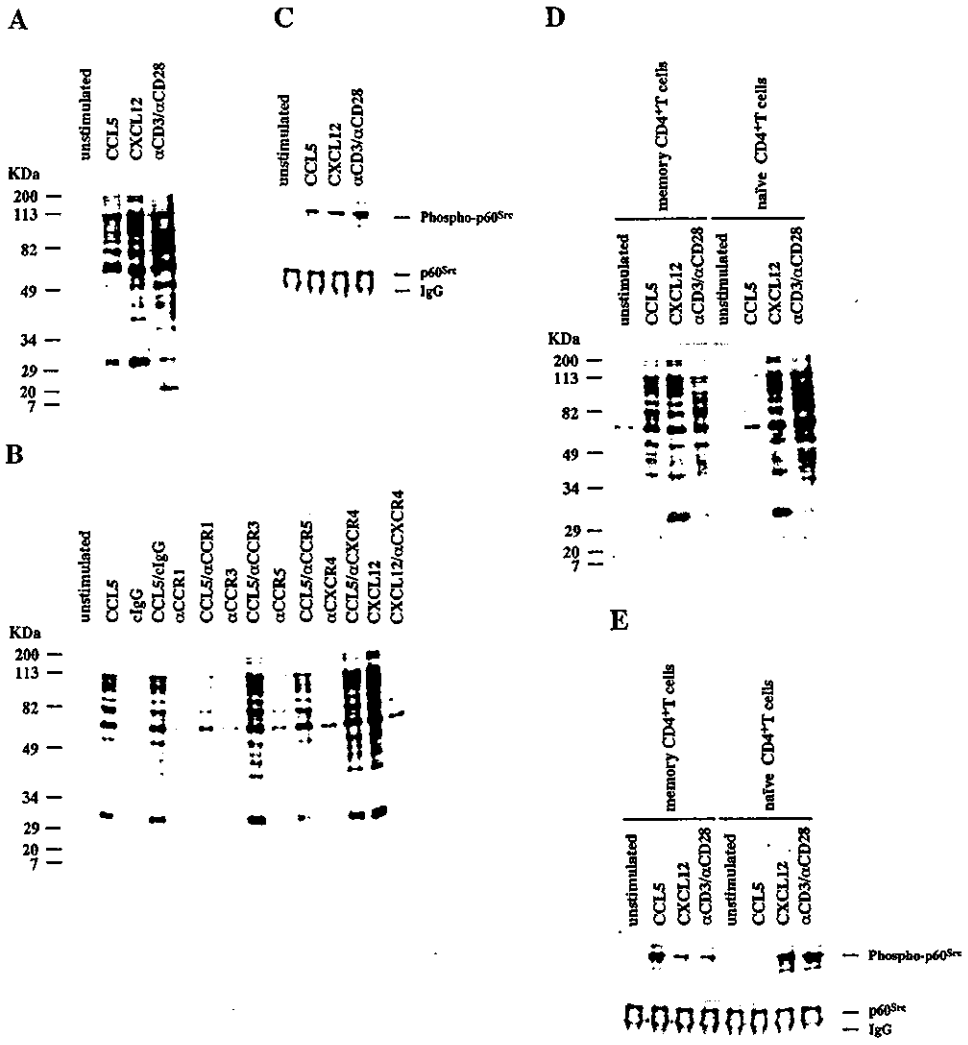

FIGURE 4. Chemokine-induced protein tyrosine phosphorylation events in memory and naive $CD4^+$ T cells. *A* and *C*, Total $CD4^+$ T cells were unstimulated or stimulated with CCL5, CXCL12, or mAbs to CD3 and CD28. *B*, Total $CD4^+$ T cells were unstimulated or stimulated with CCL5, cIgG, CCL5, and cIgG; anti-CCR1 mAb, CCL5, and anti-CCR1 mAb; anti-CCR3 mAb, CCL5, and anti-CCR3 mAb; anti-CCR5 mAb, CCL5, and anti-CCR5 mAb; anti-CXCR4 mAb, CCL5, and anti-CXCR4 mAb; CXCL12; or CXCL12 and anti-CXCR4 mAb. *D* and *E*, Memory and naive $CD4^+$ T cells were unstimulated or stimulated with CCL5, CXCL12, or mAbs to CD3 and CD28. Total cell lysates (*A*, *B*, and *D*) and immunoprecipitates obtained with Abs to $p60^{Src}$ (*C* and *E*) were analyzed by Western blotting with anti-pTyr mAb (phosphoproteins) (*A–E*) or the stated Abs to ensure that similar amounts of protein were present in each sample (*C* and *E*). The results are representative of 10 experiments.

$p60^{Src}$ in memory $CD4^+$ T cells but not in naive $CD4^+$ T cells (Fig. 4*E*). On the other hand, the level of the activation of $p60^{Src}$ was higher in naive $CD4^+$ T cells than in memory $CD4^+$ T cells following stimulation with CXCL12 or a combination of mAbs to CD3 and CD28 (Fig. 4*E*).

To address the CCL5-induced activation status of other PTKs including ZAP-70, $p125^{FAK}$, and Pyk2, which play crucial roles in ligand-induced chemotaxis of T cells (27–30), we examined their activation in memory and naive $CD4^+$ T cells following stimulation with CCL5 (Fig. 5, *A–C*). Engagement by CCL5 induced significant tyrosine phosphorylation and enzymatic activation of these PTKs in memory $CD4^+$ T cells but only a slight activation in naive $CD4^+$ T cells. We also observed that tyrosine phosphorylation of paxillin, a major cytoskeletal component in focal adhesion, was induced by CCL5 in memory $CD4^+$ T cells but not in naive $CD4^+$ T cells (Fig. 5*D*).

We further examined the level of tyrosine phosphorylation and kinase activities of a family of mitogen-activated protein kinase (MAPK), ERK2, JNK/SAPK, and $p38^{mapk}$ in memory and naive $CD4^+$ T cells following stimulation with CCL5 (Fig. 5,*E–G*). Stimulation of memory $CD4^+$ T cells with CCL5 increased tyrosine phosphorylation and kinase activities of ERK2, SAPK/JNK, and $p38^{mapk}$ compared to unstimulated cells. In contrast, engagement by CCL5 resulted in a weaker activation of these MAPKs in naive $CD4^+$ T cells than in memory $CD4^+$ T cells.

Expressions of $G_{\alpha\beta\gamma}$ complex and RGS proteins in memory and naive $CD4^+$ T cells

To address the role of CCR1 in PTK-dependent cascades, we examined the tyrosine phosphorylation of CCR1 in memory and naive $CD4^+$ cells following stimulation with CCL5. Fig. 6*A* shows that ligation by CCL5 induced tyrosine phosphorylation of CCR1 in memory $CD4^+$ T cells, whereas little tyrosine phosphorylation was observed in naive $CD4^+$ T cells.

Chemokine receptors constitutively couple with various sets of heterotrimeric G protein subunits, including G_α and $G_{\beta\gamma}$ complex, and ligation by the appropriate chemokines induces a dissociation of these subunits from GPCRs (29–32). Subsequently, the G_α subunit acts as a GTPase to regulate various downstream signaling cascades while the $G_{\beta\gamma}$ complex mediates *Ras* and *Rac1*-dependent MAPK activation via a PTK-dependent pathway (26, 27, 31–34). CCR1 reportedly coupled with $G_{i\alpha}$ or $G_{q\alpha}$ as well as various sets of $G_{\beta\gamma}$ complex (34), while CXCR4 was associated with $G_{i\alpha}$ and $G_{\beta\gamma}$ complex (35). To establish if there was any difference in the expression of the G_α subunit and $G_{\beta\gamma}$ complex between memory and naive $CD4^+$ T cells, we examined the intracellular expression levels of $G_{i\alpha}$, $G_{q\alpha}$, and $G_{\beta\gamma}$ complex. Fig. 6*B* shows that there was little or no difference in the expression levels between the cell types.

Proteins of the RGS family act as GTPase-activating proteins to accelerate GTP hydrolysis by the G_α subunit, leading to a negative

T cells with CCL5, but not CCL12, significantly impaired the binding of our anti-CCR1 mAb to the cells (Fig. 2*A*). These results indicate that our anti-CCR1 mAb specifically recognized CCR1 expressed on the cell surface in memory and naive $CD4^+$ T cells.

We further examined the effect of the mAbs blocking CCRs and CXCR on the specific binding of memory and naive $CD4^+$ T cells to ^{125}I-labeled CCL5 (Fig. 2*B*). Anti-CCR1 mAb, but not mAb to CCR3 and CXCR4, significantly inhibited specific binding of ^{125}I-labeled CCL5 to memory and naive $CD4^+$ T cells as well as $CD4^+$ T cells, while anti-CCR5 mAb partly suppressed this binding to memory $CD4^+$ T cells and total $CD4^+$ T cells, but not to naive $CD4^+$ T cells. Furthermore, the extent of the binding of ^{125}I-labeled CCL5 to anti-CCR5 mAb-treated memory $CD4^+$ T cells was similar to that of naive $CD4^+$ T cells. These results indicate that CCR1 acts as a major functional receptor for CCL5 in memory and naive $CD4^+$ T cells.

Chemokine responsiveness of memory and naive $CD4^+$ T cells

To address the features of chemokine responsiveness in memory and naive $CD4^+$ T cells, we examined the chemotactic migratory responses of these cells to CCL3, CCL5, or CXCL12. Fig. 3*A* shows that memory $CD4^+$ T cells vigorously responded to CCL3 and CCL5, whereas these chemokines caused little response of naive $CD4^+$ T cells. On the other hand, CXCL12 caused a greater attraction of naive $CD4^+$ T cells than memory $CD4^+$ T cells.

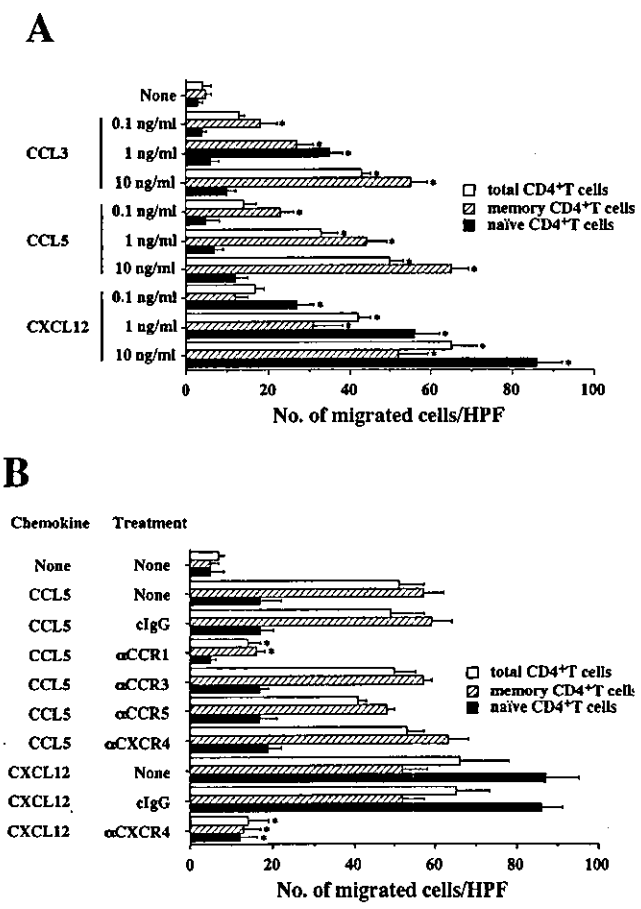

FIGURE 3. Chemokine responsiveness of memory and naive $CD4^+$ T cells. *A*, Total, memory, and naive $CD4^+$ T cells were assayed for chemotaxis to CCL3, CCL5, or CCL12. The data are expressed as the number of migrated cells/HPF. *, Value of $p < 0.001$ (compared with cells migrated to medium alone by Student's paired *t* test). *B*, Total, memory, and naive $CD4^+$ T cells were pretreated without or with the cIgG or stated mAb and then assayed for chemotaxis to CCL5 or CCL12. The data are expressed as the number of migrated cells/HPF. *, Value of $p < 0.001$ (compared with cells migrated to chemokines by Student's paired *t* test). The results are representative of 20 experiments.

To elucidate the role of CCRs in CCL5-induced chemotaxis of memory and naive $CD4^+$ T cells, we examined the effect of mAbs to block CCR1, CCR3, CCR5, and CXCR4 on the chemotaxis of these subsets to CCL5 and CXCL12 (Fig. 3*B*). The chemotactic migratory responses of memory $CD4^+$ T cells as well as total $CD4^+$ T cells to CCL5 were significantly inhibited by anti-CCR1 mAb, while anti-CCR5 mAb caused only a slight suppression of these responses. In addition, a combination of mAbs to CCR1 and CCR5 completely inhibited their responses (data not shown). In contrast, mAbs to CCR3 and CXCR4 did not suppress CCL5-induced chemotaxis. Similar results were observed for the effect of these mAbs on CCL3-induced chemotaxis of memory $CD4^+$ T cells as well as total $CD4^+$ T cells (data not shown). We also observed that anti-CXCR4 mAb significantly inhibited CXCL12-induced chemotaxis of memory and naive $CD4^+$ T cells as well as total $CD4^+$ T cells. These results indicate that CCR1 plays a crucial role in the chemotaxis of memory $CD4^+$ T cells to CCL3 and CCL5.

Different chemokine-induced signaling events in memory and naive $CD4^+$ T cells

The engagement of chemokine receptors by their respective chemokines increases the tyrosine phosphorylation of targeted intracellular proteins in various cell types, and these intracellular events appear to be crucial to the chemotactic migratory responses of these cells (26–31). CCL5 induced tyrosine phosphorylation of various intracellular proteins in total $CD4^+$ T cells, and the pattern of this event was distinct from that of cells stimulated with CXCL12 or mAbs to CD3 and CD28 (Fig. 4*A*). Furthermore, mAbs to CCR1 and CCR5, but not mAbs to CCR3 and CXCR4, inhibited CCL5-induced tyrosine phosphorylation, and anti-CCR1 mAb caused a greater suppression than anti-CCR5 mAb in total $CD4^+$ T cells (Fig. 4*B*). Similar results were observed for the effect of these mAbs on the CCL3-induced tyrosine phosphorylation of total $CD4^+$ T cells (data not shown). We also observed that anti-CXCR4 mAb completely inhibited CXCL12-induced tyrosine phosphorylation in total $CD4^+$ T cells (Fig. 4*B*).

The results suggest that a simple absence of CCR5 may not be the reason for the hyporesponsiveness of naive $CD4^+$ T cells to CCL5, because CCR1 played a crucial role in the ligand binding and the ligand-induced chemotaxis (Figs. 1–3). To clarify the molecular mechanism responsible for the distinct difference in responsiveness to CCL5 between memory and naive $CD4^+$ T cells, we examined the potential involvement of tyrosine phosphorylation events in the chemokine responsiveness of these cell types (Fig. 4*D*). Stimulation with CCL5 induced tyrosine phosphorylation of various intracellular proteins in memory $CD4^+$ T cells but not in naive $CD4^+$ T cells. In contrast, stimulation with CXCL12 or a combination of mAbs to CD3 and CD28 caused a more potent tyrosine phosphorylation of several intracellular proteins in naive $CD4^+$ T cells than in memory $CD4^+$ T cells.

To examine the difference in the activation of protein tyrosine kinases (PTKs) between memory and naive $CD4^+$ T cells following stimulation with various stimuli, we tested their tyrosine phosphorylation level and kinase activity of $p60^{Src}$. Stimulation with CCL5 or CXCL12 caused a tyrosine phosphorylation of $p60^{Src}$, and levels of activation were slightly lower than those in cells stimulated with mAb to CD3 and CD28 in the total $CD4^+$ T cell population (Fig. 4*C*). Furthermore, CCL5 induced activation of

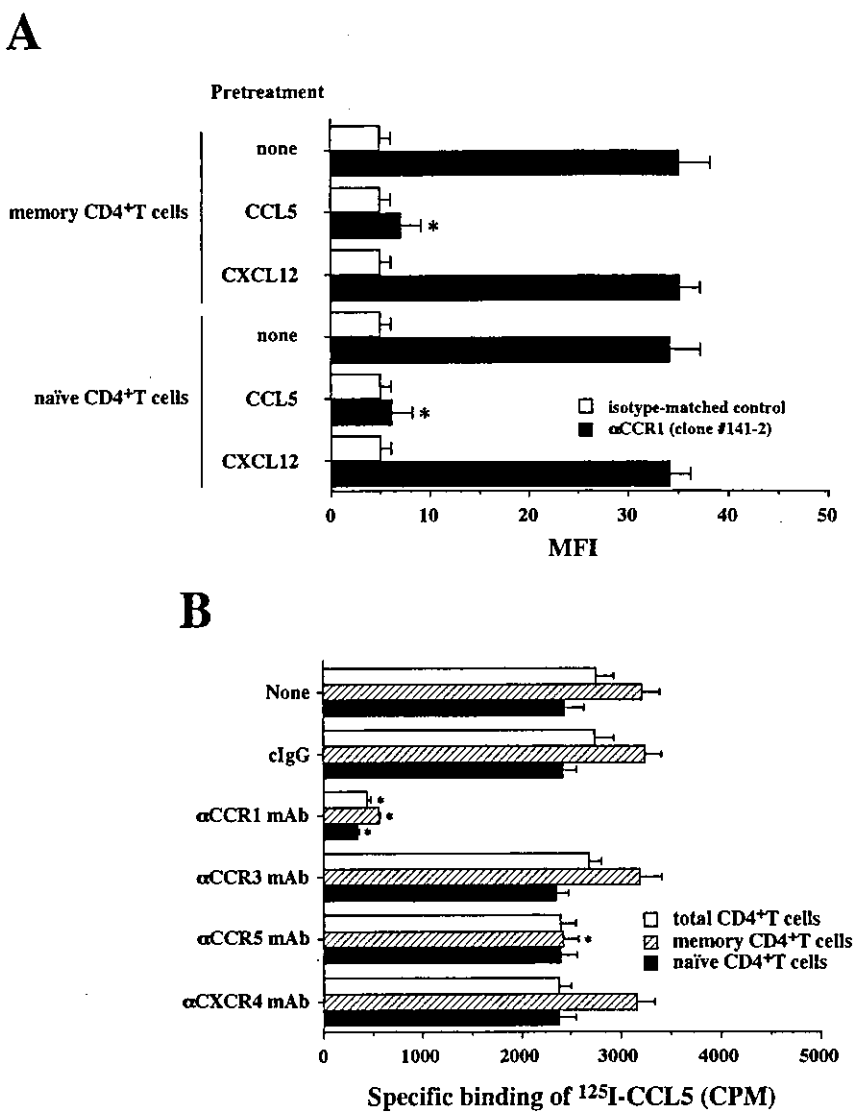

FIGURE 2. Binding activity of memory and naive $CD4^+$ T cells to CCL5. *A*, Memory and naive $CD4^+$ T cells were pretreated with or without CCL5 or CXCL12. Subsequently, cells were stained with anti-CCR1 mAb (clone 141-2) or isotype-matched mAbs, and their cell surface expressions were analyzed by FACS. Data were expressed as MFI. *, Value of $p < 0.001$ (compared with the respective untreated cells by Student's paired t test). The results are representative of 20 experiments. *B*, Memory and naive $CD4^+$ T cells were pretreated without or with the stated mAb, and then cells were incubated with ^{125}I-labeled CCL5 (~0.1 nM) in the presence of an excess of unlabeled CCL5 (10 nM). The results are representative of five experiments performed in duplicate. *, Value of $p < 0.001$ (compared with the respective untreated cells by Student's paired t test).

cells (Ref. 16 and Fig. 1*A*). In addition, our anti-CCR1 mAb (MFI = 216) showed a higher staining of CCR1 in CCR1-expressing transfectants than the previously established anti-CCR1 mAb (clone 53504.111; MFI = 134) (Fig. 1*A*).

We tested the expression level of CCR1 (for CCL3 and CCL5) in $CD4^+$ T cells (total $CD4^+$ T cells) by flow cytometry with our anti-CCR1 mAb using monocytes for comparison because the expression level of CCR1 in PB $CD4^+$ T cells was controversially reported (9, 10, 16). Figure 1*B* shows that the expression level of CCR1 in total $CD4^+$ T cells (MFI = 34) was lower than that in monocytes (MFI = 58).

A series of studies have shown that CCL3 and CCL5 selectively attract a subset of memory T cells (5, 7, 9, 16). To elucidate the molecular mechanism underlying the responsiveness of $CD45RO^+$ $CD4^+$T cells (memory phenotype) and $CD45RA^+CD4^+$ T cells (naive phenotype) to CCL3 and CCL5, these subsets were isolated from PB $CD4^+$ T cells (total $CD4^+$ T cells) (Fig. 1*C*), and the expressions of CCR1, CCR3 (for CCL5 and CCL11/eotaxin), CCR5 (for CCL3 and CCL5), and CXCR4 (for CXCL12/stromal cell-derived factor (SDF)-1α) were examined (Fig. 1*D*). Flow cytometric analysis revealed that memory and naive $CD4^+$ T cells highly expressed CCR1 at similar levels, whereas the expression level of CXCR4 was higher in naive $CD4^+$ T cells than in memory $CD4^+$ T cells. Furthermore, CCR5 was only expressed in memory $CD4^+$ T cells at low levels. We also observed that there was little or no expression of CCR3 on the cell surface of either cell type.

We also examined the transcriptional expressions of CCR1, CCR5, and CXCR4 in memory and naive $CD4^+$ T cells by semiquantitative RT-PCR analysis (Fig. 1*E*). The transcriptional expression level of CCR1 in memory $CD4^+$ T cells was similar to that in naive $CD4^+$ T cells, and these expression levels were lower than that in monocytes. Furthermore, the expression level of CCR5 transcript was significantly higher in memory $CD4^+$ T cells than in naive $CD4^+$ T cells, and this expression level was similar to that in monocytes. In addition, the transcriptional expression of CXCR4 was higher in naive $CD4^+$ T cells than in monocytes and memory $CD4^+$ T cells, and monocytes showed a higher expression of CXCR4 transcript than memory $CD4^+$ T cells. We also observed that CD14 transcript, but not TCR transcript, was not detected in the preparations of memory and naive $CD4^+$ T cells, whereas CD14 transcript was exclusively detected in the preparation of monocytes (Fig. 1*E*). These results exclude the possibility that the CCR1 mRNA of monocytes is the source for the PCR results with these T cells.

To address the specific binding of anti-CCR1 mAb with CCR1 expressed on the cell surface in memory and naive $CD4^+$ T cells, we examined the blocking effect of CCL5 on the binding of anti-CCR1 mAb to the cells. Pretreatment of memory and naive $CD4^+$

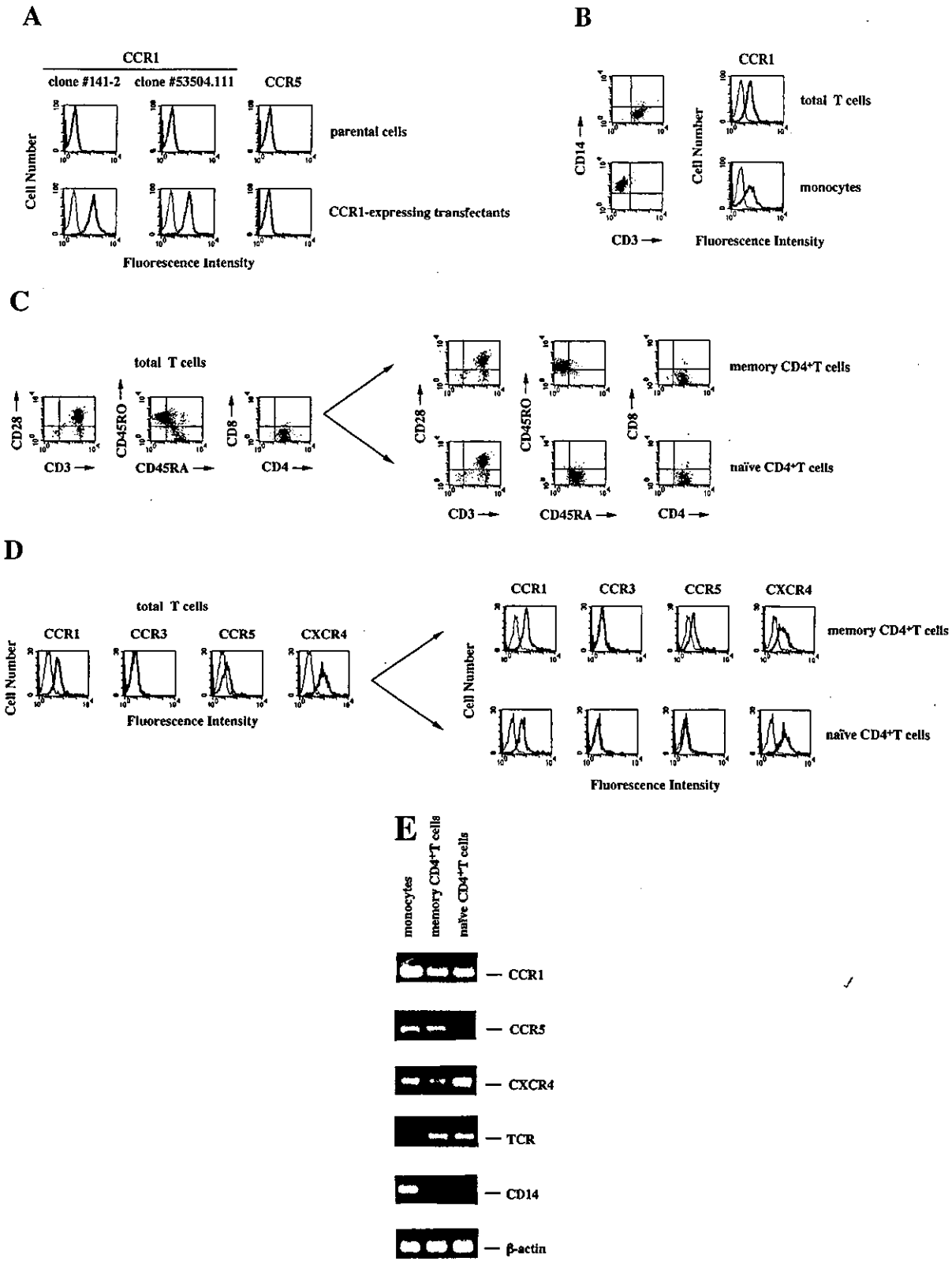

FIGURE 1. Chemokine receptor expression in memory and naive $CD4^+$ T cells. *A*, Cells were stained with anti-CCR1 mAb (clone 141-2 or clone 53504.11) or isotype-matched mAbs, and their cell surface expressions were analyzed by FACS. Data are represented by histograms in which cells were stained with the stated mAbs (thick lines) or isotype-matched mAbs (thin lines). *B*, Cells were stained with the mAbs to CD3 plus CD14, anti-CCR1 mAb (clone 141-2), or isotype-matched mAbs, and their cell surface expressions were analyzed by FACS. Data are represented by dot plots (*left*) and histograms (*right*) in which cells were stained with the stated mAbs (thick lines) or isotype-matched mAbs (thin lines). *C* and *D*, Cells were stained with the stated mAbs or isotype-matched mAbs, and their cell surface expressions were analyzed by FACS. Data are represented by dot plots (*C*) and histograms (*D*) in which cells were stained with the stated mAbs (thick lines) or isotype-matched mAbs (thin lines). *E*, RNA was extracted from monocytes, memory and naive $CD4^+$ T cells obtained from same individual used in C and D, and the mRNA expressions of CCR1, CCR5, and CXCR4 were evaluated by semiquantitative RT-PCR. PCR products for CCR1 (440 bp), CCR5 (1117 bp), CXCR4 (810 bp), TCR (386 bp), CD14 (535 bp), and β-actin (645 bp) are shown. The results of RT-PCR for β-actin demonstrate the loading of equal amounts of DNA on the gel.

anti-mouse IgG mAb-conjugated immunomagnetic beads (Dynal Biotech, Oslo, Norway). The purity of monocytes was >98% by FACS analysis with anti-CD14-FITC (BD Biosciences, Mountain View, CA). CCR1-expressing transfectants were established by the transfection of cDNA for PCR-amplified CCR1 cDNA into mouse preB cell lymphoma B300-19 (parental cells) (17), and maintained in RPMI 1640 (Sigma-Aldrich) supplemented with antibiotic-antimycotic (Life Technologies, Rockville, MD) and 10% heat inactivated FCS (Life Technologies).

Flow cytometry

Cells were analyzed as described previously (16–18), using anti-CD3-FITC, anti-CD4-FITC, anti-CD8-PE, anti-CD28-PE, anti-CD45RA-FITC, anti-CD45RO-PE, anti-CCR5-FITC, anti-CXCR4-biotin, avidin-FITC (all from BD PharMingen), anti-CCR1-biotin (clone 141-2), anti-CCR1-biotin (clone 53504.111; R&D Systems, Minneapolis, MN), or anti-CCR3-biotin (17). Signals were acquired on a FACSCalibur flow cytometer (BD Biosciences) with CellQuest software (BD Biosciences). In some experiments, the expression levels of cell surface products were expressed as mean fluorescence intensity (MFI).

Blocking staining of CCR1 with CCL5 in T cell subsets

Cells were untreated (medium alone) or treated with CCL5 or CXCL12 (500 ng/ml) at 4°C for 30 min, and washed twice with cold PBS. Subsequently, cells were stained with anti-CCR1 mAb (clone 141-2), and the cell surface expression level of CCR1 was analyzed by flow cytometry as described above.

Semiquantitative RT-PCR

Total RNA (5 μg) from each sample (5×10^6) was isolated using TRIzol LS reagent (Life Technologies). Single-stranded cDNA (20 μl) was synthetized using 1 μg of total RNA and the first strand cDNA kit (SuperScript Preamplication System; Life Technologies) containing 0.5 mM concentrations of each dNTP, 0.5 μg of oligo$(dT)_{12-18}$ primers, 20 mM Tris-HCl (pH 8.4), 50 mM KCl, 5 mM $MgCl_2$, 10 mM dithiothreitol, 40 U RNase inhibitor, 50 U of Superscript II reverse transcriptase, and 2 U RNase H according to the manufacturer's instructions. Subsequently, amplification of each cDNA (1 μl) was performed with a SuperTaq Premix kit (Sawady Technology, Tokyo, Japan) using specific primers as follows: CCR1 (19), 5′-TCCTCACGAAAGCCTACGAGAGTGGAAGC-3′ and 5′-CCACGG AGAGGAAGGGGAGCCATTTAAC-3′; CCR5 (19), 5′-GGTGGAACA AGATGGATTAT-3′ and 5′-CATGTGCACAACTCTGACTG-3′, CXCR4 (19), 5′-CTGAGAAGCATGACGGACAAGTACAGGCT-3′ and 5′-CAGA TGAATGTCCACCTCGCTTTCCTTTGG-3′; TCR (20), 5′-CCGAGGTC GCTGTGTTTGAGCCAT-3′ and 5′-GCTCTACCCCAGGCCTCGGC-3′; CD14 (21), 5′-GCTGGACGATGAAGATTTCC-3′ and 5′-ATTGTCAGAC AGGTCTAGGC-3′. Specific primers for β-actin (Toyobo, Osaka, Japan) were also used for amplification. To activate DNA polymerase, preheating (95°C for 5 min) was performed. The reaction mixture was subjected to 30 cycles of PCR with the following conditions: CCR1, CXCR4, TCR, CD14, and β-actin, 95°C for 30 s, 55°C for 30 s, and 72°C for 1 min; CCR5, 94°C for 1 min, 55°C for 1 min, and 72°C for 1 min. Following these procedures, a final extension (72°C for 3 min) was performed. The expected sizes of PCR products for CCR1, CCR5, CXCR4, TCR, CD14, or β-actin was 440, 1117, 810, 386, 535, or 645 bp, respectively. Contamination with genomic DNA was routinely checked by omitting the Superscript II during reverse transcription. Amplification without cDNA was also carried out to assess later contaminations. The PCR products were analyzed by electrophoresis through 2% agarose gels and visualized under UV light after ethidium bromide staining.

Assay for chemotaxis

The chemotaxis of $CD4^+$ T cells and their subsets to CCL3, CCL5, and CXCL12 (1–100 ng/ml; PeproTech, London, U.K.) was determined as described previously (16). The data are expressed as the number of migrated cells per high-power field (HPF).

Western blotting and immune complex kinase assay

Cells (4×10^6) were untreated or stimulated with CCL5, CXCL12 (10 ng/ml), or a combination of immobilized mAbs to CD3 and CD28 (all from BD PharMingen) (18) for 3 min at 37°C, and total cell lysates were collected (18). Total cell lysates or immunoprecipitates obtained with an Ab to $p60^{Src}$, ZAP-70, $p125^{FAK}$, Pyk2, paxillin, or CCR1 (all from Santa Cruz Biotechnology, Santa Cruz, CA) were fractionated by 12% SDS-PAGE, transferred onto polyvinylidene difluoride membranes (Millipore, Bedford, MA) and probed with HRP-conjugated anti-phosphotyrosine (pTyr) mAb (clone RC20; Transduction Laboratories, Lexington, KY), $G_{i\alpha}$, $G_{q\alpha}$, regulator of G protein signaling (RGS)1, RGS3, RGS4, actin (all from Santa Cruz Biotechnology), or G$\beta\gamma$ complex (CytoSignal, Irvine, CA). Blots were visualized by ECL (New England Biolabs, Beverly, MA). To ensure that similar amounts of respective proteins were present in each sample, the same membrane was stripped off, reprobed with the stated Abs, and developed with HRP-conjugated secondary Abs (Santa Cruz Biotechnology) by ECL. In another experiment, immunoprecipitate obtained with Abs to ZAP-70, $p125^{FAK}$, or Pyk2 from total cell lysates (10^7 cells) was subjected to in vitro kinase assay with enolase (Sigma-Aldrich) as a substrate as described previously (18). Immunoblotting and the in vitro kinase assay of extracellular signal-regulated kinase (ERK)2, stress-activated protein kinase (SAPK)/c-Jun N-terminal kinase (JNK), or $p38^{mapk}$ were performed with respective kits (New England Biolabs) according to the manufacturer's instructions (18).

Whole cell binding assay

The binding of ^{125}I-labeled CCL5 to targeted cells was assayed as reported previously (22, 23). In brief, cells (10^5/sample) were resuspended in 200 μl of binding medium (RPMI 1640/1% BSA) and incubated for 1 h at room temperature with ^{125}I-labeled CCL5 (~0.1 nM; specific radioactivity = 2200 Ci/mmol; NEN Life Science Products, Boston, MA) in the presence of an excess of competitive unlabeled (cold) CCL5 (10 nM). Cells were then spun (12,000 rpm for 1 min) through an 800-μl cushion of 10% (w/v) sucrose in PBS. The pellet was dried and then measured with an automatic gamma counter (ARC-380; Aloka, Tokyo, Japan).

Membrane binding assay

Cell membranes were prepared by lysis of cells (4×10^6) in a lysis buffer (10 mM HEPES (pH 7.5), 3 mM $MgCl_2$, 2 mM EDTA, 40 μg/ml PMSF, 10 μg/ml leupeptin, 2 μg/ml pepstain A, and 2 μg/ml aprotinin). After homogenization and sonication, they were centrifuged at $1,000 \times g$ for 10 min, and the supernatant was transferred into Beckman tubes and ultracentrifuged at $150,000 \times g$ for 30 min at 4°C. Membrane binding assay was performed as reported previously (24). In brief, cell membranes were preincubated with various concentrations (10^{-7}–10^{-3} nM) of GTP-γS (Sigma-Aldrich) for 30 min at 37°C. Subsequently, cell membranes were incubated in a 96-well plate with ^{125}I-labeled CCL5 (~0.1 nM) in the presence of an excess of competitive unlabeled (cold) CCL5 (10 nM) in a total volume of 100 μl of binding buffer (50 mM HEPES (pH 7.2), 5 nM $MgCl_2$, 1 mM $CaCl_2$, 0.5% BSA, 0.002% sodium azide, and protease inhibitors). Following an incubation for 90 min at 24°C, the membranes were centrifuged at 2500 rpm for 10 min. The supernatant was decanted, 100 μl of binding buffer (4°C) containing 0.5 M NaCl was added, and the membranes were transferred to a microtube. Following two additional rinses, they were transferred to scintillation vials, and then measured with an automatic gamma counter.

Assay for GTP-GDP exchange

Assay for GTP-GDP exchange was performed as reported previously (25). In brief, cell membranes were transferred into a buffer containing 10 mM HEPES, 3 mM $MgCl_2$, and 2 mM EDTA. For preparation of anti-G protein Ab- or IgG-coated immunomagnetic beads, anti-rabbit IgG mAb-conjugated immunomagnetic beads (Dynal Biotec) were incubated for 2 h at 4°C with rabbit anti-G protein or rabbit IgG in a PBS containing 1% BSA. Subsequently, cell membranes incubated first with CCL5 or CXCL12 (10 ng/ml) were added to the GTP binding buffer (20 mM HEPES/NaOH (pH 7.4), 0.1 mM EDTA, 0.125 mM $MgCl_2$) plus [γ-^{35}S]GTP (specific radioactivity = 1250 Ci/mmol; NEN Life Science Products) and then mixed with anti-G protein- or IgG-coated beads, washed with PBS buffer plus 0.05% Tween 20, and suspended in the scintillation mixture. They were transferred to scintillation vials and counted in a liquid scintillation counter (LSC-5100; Aloka).

Statistical analysis

All analyses for statistically significant differences were performed with the Student's paired t test. Values of $p < 0.001$ were considered significant. Results were expressed as the mean values ± SD.

Results

Chemokine receptor expression of memory and naive $CD4^+$ T cells

We have previously generated an mAb to human CCR1 (clone 141-2), and this mAb showed the specificity and the reliability of CCR1 staining using CCR1-expressing transfectants and parental

An Abortive Ligand-Induced Activation of CCR1-Mediated Downstream Signaling Event and a Deficiency of CCR5 Expression Are Associated with the Hyporesponsiveness of Human Naive CD4$^+$ T Cells to CCL3 and CCL5[1]

Katsuaki Sato,[2]* Hiroshi Kawasaki,† Chikao Morimoto,† Naohide Yamashima,‡ and Takami Matsuyama*

Human memory CD4$^+$ T cells respond better to inflammatory CCLs/CC chemokines, CCL3 and CCL5, than naive CD4$^+$ T cells. We analyzed the regulatory mechanism underlying this difference. Memory and naive CD4$^+$ T cells expressed similarly high levels of CCR1; however, CCR5 was only expressed in memory CD4$^+$ T cells at low levels. Experiments using mAbs to block chemokine receptors revealed that CCR1 functioned as a major receptor for the binding of CCL5 in memory and naive CD4$^+$ T cells as well as the ligand-induced chemotaxis in memory CD4$^+$ T cells. Stimulation of memory CD4$^+$ T cells with CCL5 activated protein tyrosine kinase-dependent cascades, which were significantly blocked by anti-CCR1 mAb, whereas this stimulation failed to induce these events in naive CD4$^+$ T cells. Intracellular expressions of regulator of G protein signaling 3 and 4 were only detected in naive CD4$^+$ T cells. Pretreatment of cell membrane fractions from memory and naive CD4$^+$ T cells with GTP-γS inhibited CCL5 binding, indicating the involvement of G proteins in the interaction of CCL5 and its receptor(s). In contrast, CCL5 enhanced the GTP binding to $G_{i\alpha}$ and $G_{q\alpha}$ in memory CD4$^+$ T cells, but not in naive CD4$^+$ T cells. Thus, a failure of the ligand-induced activation of CCR1-mediated downstream signaling event as well as a deficiency of CCR5 expression may be involved in the hyporesponsiveness of naive CD4$^+$ T cells to CCL3 and CCL5. *The Journal of Immunology,* **2002, 168: 6263–6272.**

Chemokines are part of a family of small molecular mass proteins (8–10 kDa) that regulate the migration and activation of leukocytes (1–3). Chemokines have been implicated in the regulation of normal immune response and inflammation as well as certain physiological and pathogenic processes, including hematopoiesis, angiogenesis, allergy, autoimmune disorders, and infectious diseases (1–3). Responses to chemokines are mediated by a family of single-chain, seven-helix membrane-spanning receptors coupled to heterotrimeric guanine nucleotide-binding protein (G protein-coupled receptor (GPCR)[3]) (1–3). There are two major chemokine subfamilies (CCLs/CC chemokines and CXCLs/CXC chemokines), distinguished based on the number of cysteines and the spacing between the first two cysteines. Their receptors also comprise two major groups: CCR1–10 bind CCLs, and CXCR1–5 bind CXCLs (1–3). In addition, certain chemokines appear to act on more than one receptor type in vitro (1–3).

Evidence is accumulating that the interaction between chemokines and their receptors is crucial for the selective migration of circulating peripheral blood (PB) T cells to sites of inflammatory reactions or secondary lymphoid tissues (2–5). Patterns of chemokine receptor expression and the responsiveness of PB T cells are thought to be correlated with the properties of their subsets, including memory vs naive phenotype (4–11) and Th1 vs Th2 (12–15). Previous studies have shown that certain inflammatory CCLs and CXCLs selectively attract a subset of memory CD4$^+$ T cells (4–11). Closer analysis of this feature revealed that the distinct chemotactic behavior of memory and naive CD4$^+$ T cells to certain chemokines, including CCL3/macrophage-inflammatory protein-1α and CCL5/RANTES, is not simply explained by the expression levels of their receptors (CCR1 and CCR5), although the responsiveness of these subsets to other CCLs and CXCLs is correlated with the levels of appropriate chemokine receptors (9, 16).

In this study, we examined the role of CCRs and their downstream signaling events in the responsiveness of memory and naive CD4$^+$ T cells to CCL3 and CCL5.

Materials and Methods

Preparation and culture of T cells, their subsets, and monocytes

CD4$^+$CD45RO$^+$ T cells and CD4$^+$CD45RA$^+$ T cells were purified from PBMCs as described previously (16). Purity (>97% CD3$^+$CD4$^+$ CD45RAO$^+$ cells and >97% CD3$^+$CD4$^+$CD45RA$^+$ cells) was tested by FACS analysis. In some experiments, cells were untreated or treated with various concentrations (0.01–1 μg/ml) of blocking mAbs to CCR1 (clone 141-2; Ref. 17), CCR3 (17), CCR5 (BD PharMingen, San Diego, CA), CXCR4 (BD PharMingen), or control IgG (cIgG; Sigma-Aldrich, St. Louis, MO) for 30 min at 4°C, and then used for subsequent experiments. For preparation of monocytes, cells were negatively selected with mAbs to CD3, CD19, and CD56 (all from BD PharMingen) in combination with

*Department of Immunology and Medical Zoology, School of Medicine, Kagoshima University, Sakuragaoka, Kagoshima, Japan; †Department of Clinical Immunology and AIDS Research Center, and ‡Department of Advanced Medical Science, Institute of Medical Science, University of Tokyo, Tokyo, Japan

Received for publication October 29, 2001. Accepted for publication April 26, 2002.

The costs of publication of this article were defrayed in part by the payment of page charges. This article must therefore be hereby marked *advertisement* in accordance with 18 U.S.C. Section 1734 solely to indicate this fact.

[1] This work was supported by Grants-in-Aid for Scientific Research from the Ministry of Education, Science and Culture of Japan (Grant 13218027 to K.S. and H.K.), the Naito Foundation (to K.S.), Nagao Memorial Fund (to K.S.) and Kodama Memorial Fund Medical Research (to K.S.).

[2] Address correspondence and reprint requests to Dr. Katsuaki Sato, Department of Immunology and Medical Zoology, School of Medicine, Kagoshima University, 8-35-1 Sakuragaoka, Kagoshima City, Kagoshima 890-8520, Japan. E-mail address: katsuaki@m3.kufm.kagoshima-u.ac.jp

[3] Abbreviations used in this paper: GPCR, G protein-coupled receptor; ERK, extracellular signal-regulated kinase; HPF, high-power field; MAPK, mitogen-activated protein kinase; PB, peripheral blood; PTK, protein tyrosine kinase; pTyr, phosphotyrosine; RGS, regulator of G protein signaling; SAPK, stress-activated protein kinase; JNK, c-Jun N-terminal kinase; SDF, stromal cell-derived factor; MFI, mean fluorescence intensity; cIgG, control IgG.

0022-1767/02/$02.00